AECD-3928

RADIATION EFFECTS QUARTERLY PROGRESS REPORT JANUARY—MARCH, 1954

EDITED BY:

F. E. FARIS

Declassification date: December 9, 1955

Photostat Price $ 7.80

Microfilm Price $ 3.30

Available from the
Office of Technical Services
Department of Commerce
Washington 25, D. C.

ATOMIC ENERGY RESEARCH DEPARTMENT
NORTH AMERICAN AVIATION, INC.
P. O. BOX 309 DOWNEY, CALIFORNIA

SUBMITTED: MAY 24, 1954

ISSUE DATE

AUGUST 15, 1954

CONTRACT AT 11-1-GEN-8

619-1

TABLE OF CONTENTS

619-2

LIST OF FIGURES

LIST OF FIGURES (Continued)

Previous Quarterly Progress Reports in this Series

NAA-SR-229	Solid State and Irradiation Physics Quarterly Progress Report October-December, 1952
NAA-SR-251	Solid State and Irradiation Physics Quarterly Progress Report January-March, 1953
NAA-SR-268	Solid State and Irradiation Physics Quarterly Progress Report April-June, 1953
NAA-SR-286	Radiation Effects Quarterly Progress Report July-September, 1953
NAA-SR-909	Radiation Effects Quarterly Progress Report October-December, 1953

This report is based upon studies conducted for the Atomic Energy Commission under Contract AT-11-1-GEN-8.

I. GRAPHITE

A. Thermal Conductivity of Graphite - J. E. Hove, W. P. Eatherly

As is well known, the thermal conductivity of polycrystalline graphite at low temperatures shows nearly a T^3 temperature dependence while the specific heat varies as T^2. If one employs the usual relation for a lattice heat conductor ($k \propto Cv\lambda$), graphite becomes an anomalous case since at low temperatures the relaxation path, λ, and the phonon group velocity, v, are nearly temperature independent, and the thermal conductivity, k, should have the same temperature dependence as the specific heat, C. This conclusion admittedly assumes that the thermal waves decay by boundary scattering; but any other type of scattering important at low temperature, such as that due to defects or mosaic boundaries, would be expected to decrease the dependence of k on temperature. In order to interpret the effects of radiation damage on the thermal conductivity, it is of great importance to understand the fundamental properties of the unirradiated material; and thus the cause of this anomaly in graphite is a subject of some interest.

The only published serious attempt to explain this anomaly has been made by P. G. Klemens,[1] whose work seems open to some criticism and will be discussed later. It is the present feeling of this laboratory that the explanation lies in the presence of ungraphitized carbonaceous material which forms the bond between graphite particles; and the following analysis is tentatively advanced, pending further experimental work on "single" crystals.

If one assumes the ungraphitized region to have essentially diamond-like tetravalent bonding, this region is three-dimensional in nature, as opposed to the two-dimensional character of the graphite particles. At low temperatures where the predominant thermal waves have wavelengths much greater than the size of local irregularities in the ungraphitized region, one should further be able to treat this region as an isotropic quasicontinuum. One may, therefore, assign a Debye temperature to it, which will be assumed to be of the order of the Debye temperature of diamond. If the subscript 2 refers to the two-dimensional graphitic region, and the subscript 3 to the three-dimensional non-graphitic region, the following relations should hold:

$$k_2 = \frac{1}{2} C_2 v_2 \lambda_2; \quad k_3 = \frac{1}{3} C_3 v_3 \lambda_3, \qquad \ldots(1)$$

where the symbols are the same as those used previously. Since the two mediums are in series, the total thermal conductivity is

$$\frac{1}{k} = \frac{a}{s k_2} + \frac{(1-a)}{k_3} , \qquad \ldots(2)$$

where a is the fraction of the volume of the specimen which is graphite, and s is the effective fraction of the graphitic (two-dimensional) region which is aligned parallel to the temperature gradient (i. e., parallel to the heat flow). A fraction analogous to s for the non-graphitic region would be unity, since this region has been assumed three-dimensionally isotropic. It can be immediately seen that the expression (Eq. (2)) is qualitatively what is desired, since $C_2 \propto T^2$ and $C_3 \propto T^3$. The value of k at low temperatures will be governed by the non-graphitic medium and will be nearly proportional to T^3. On the other hand the total specific heat will be just the sum of C_2 and C_3 (with appropriate weighting factors), which will behave as T^2 at low temperatures.

For a quantitative check, it is necessary to calculate theoretical expressions for C_2, C_3, v_2 and v_3, which will be functions of the Debye temperatures and the atomic volumes. The Debye temperatures will be taken as $\theta_2 = 1000°$ K, $\theta_3 = 3000°$ K; this value of θ_2 is approximately that corresponding to graphite modes with out-of-plane polarizations. With these assumptions, Eq. (2) becomes

$$k = \frac{bT^3}{T+a} \qquad \ldots(3)$$

where

$$b = \frac{S}{a} \lambda_2 ;$$

$$a = 60 \frac{(1-a)}{a} S\left(\frac{\lambda_2}{\lambda_3}\right) .$$

619-7

The values of a and s can be estimated from the magnetic susceptibility and the conductivity anisotropy, respectively. By rewriting Eq. (3) as

$$\frac{T^3}{k} = \left(\frac{a}{s\lambda_2}\right) T + 60\,(1 - a)\,\frac{1}{\lambda_3} \qquad \ldots(4)$$

it is seen that if λ_2 and λ_3 are temperature independent, a plot of T^3/k vs T should be linear, with the slope determining λ_2 and the intercept determining λ_3. Figure 1 shows such plots for AGOT-KC, AWG, and SA-25 graphites using recent data,[2] and below 40 or 50° K all types show a reasonably linear temperature dependence. The two curves for AWG represent independent measurements of different samples; the slopes are nearly equal, a result which indicates that the mean-free path of the phonons inside the graphitic particles is an experimentally reproducible quantity. The variation in the intercept could be a consequence of a variation in the void space in the ungraphitized region or of a different amount or distribution of the ungraphitized material. It is thus apparent that the present analysis is too simplified to account correctly on an absolute basis for the effect of the ungraphitized region. From the values of the slopes and intercepts of Fig. 1, the following values of the mean-free paths are obtained.

	λ_2 (Å)	λ_3 (Å)	Approximate Crystallite Size	Particle Classification
AGOT-KC	6230	2590	>3000	large
AWG(I)	2280	590	>2000	medium
AWG(II)	2160	1590	>2000	medium
SA-25	935	65	~ 500	small

The values for λ_2 are seen to be of a reasonable magnitude and to decrease as the particle and crystallite sizes decrease. In SA-25 the particles are about 3000 Å in diameter; by assuming 7 per cent of the volume to be non-graphitic (obtained from the susceptibility) and assuming this material to be uniformly distributed around spherical particles the average thickness of the non-graphitic region is found to be about 100 Å, which is of the order of λ_3 as

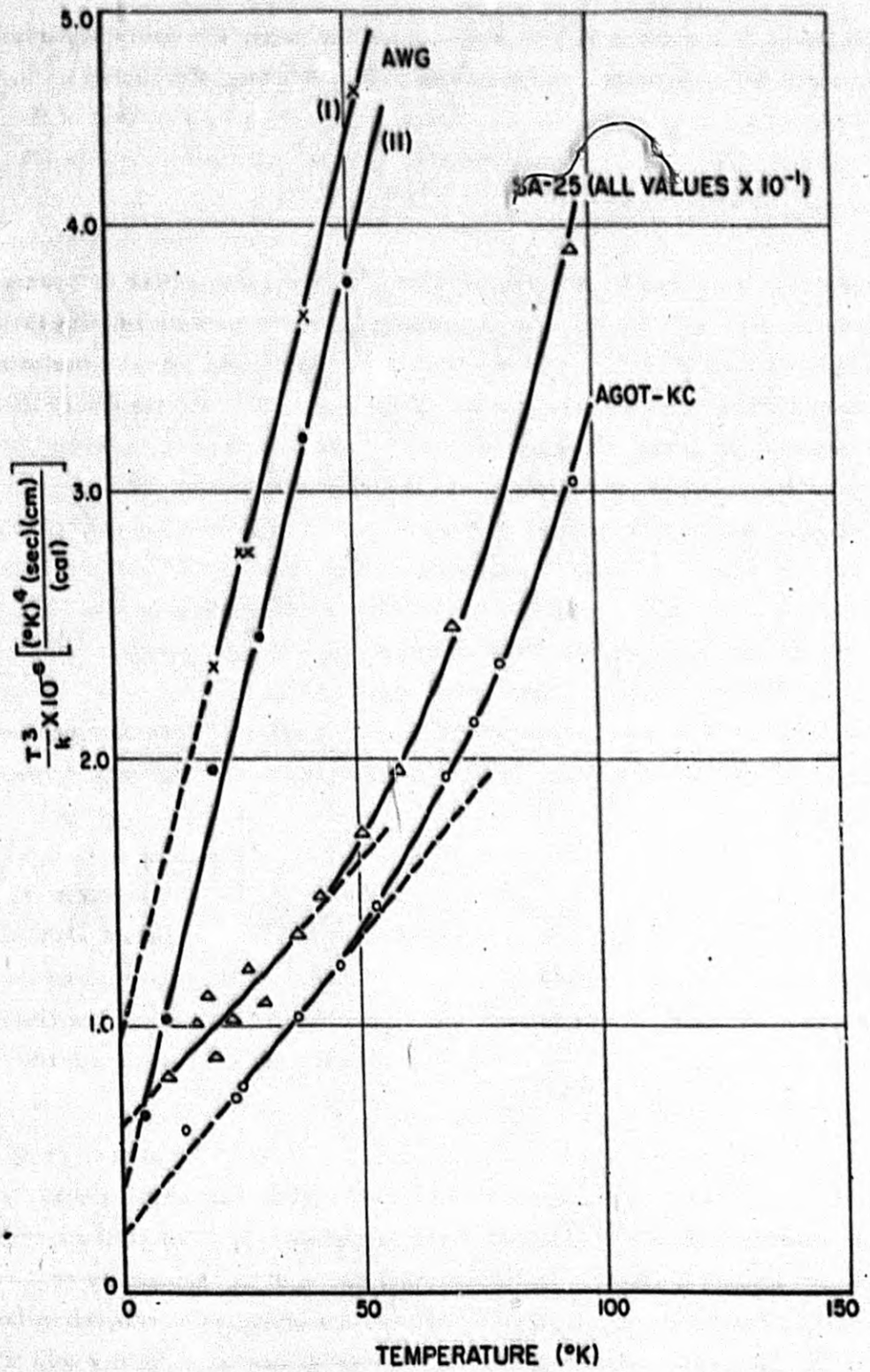

Fig. 1. Temperature Dependence of $\left[T^3/k\right]$ for Various Graphites

619-9

obtained above. For the AGOT-KC one should probably assume the particles to be cylindrical slabs with a thickness to diameter ratio of about 1:3. In the manufacturing process of KC, a coke flour is used with 60 per cent of the particles less than about 75 μ in size; if the average particle length is taken to be 50 μ, and 10 per cent of the final specimen volume is taken to be non-graphitic, the average thickness of the non-graphitic region is about 3000 Å, which again is of the same order as λ_3 obtained above. Thus, a quantitative comparison of this theory with experiment seems to yield quite reasonable results for the artifical graphites. It should be noted that the effect of the non-graphitic region on the total specific heat is negligible. If one writes $C \sim T^{\gamma}$, then the expression for γ as derived from the present analysis is

$$\gamma = 2 + 2 \times 10^{-3} \left(\frac{1 - \alpha}{\alpha}\right) T,$$

which (for $\alpha = 0.9$) give $\gamma = 2.002$ at 10° K and $\gamma = 2.02$ at 100° K. The experimental results of DeSorbo and Tyler[3] show $\gamma = 2.00 \pm 0.05$ for a temperature range of 15° K to 60° K

The results of measurements on natural (ceylon) graphite samples, when plotted as in Fig. 1, show a behavior similar to that of the artifical graphites, even though the amount of non-graphitic material is known to be very low. If 1 per cent of the volume is assumed non-graphitic, the result is a λ_2 of about 7000 Å and a λ_3 of about 150 Å. However, considerable doubt exists as to the validity of the natural-graphite data, since the specimen used has a skewed orientation as evidenced from electrical potential mappings. It is clear that additional data on graphite with little or no ungraphitized material are needed and such measurements are now being planned. Measurements on a large "single" crystal, of course, would settle the issue.

The variation of the curve in Fig. 1 from a straight line at temperatures above 50° K is presumably caused by the failure of the low-temperature specific-heat approximation (which starts to break down for graphite at around 60° K) and by an increase in the relative importance of non-boundary scattering mechanisms. The latter will lead to a temperature-dependent relaxation length. By correcting the present analysis for the specific heat variation it would thus be possible to obtain the actual temperature dependence of the relaxation lengths.

A certain ambiguity exists, however, since there are two relaxation paths (λ_2 and λ_3) to be considered. There is probably no such ambiguity in the case of radiation effects, since one would not expect the damage to change appreciably the characteristics of the non-graphitic region. Both of these problems will be considered from the two-medium viewpoint in the near future.

As mentioned previously, an article by P. G. Klemens[1] appeared recently in which an attempt was made to explain the anomalous temperature dependence of the thermal conductivity as an intrinsic property of the graphite caused by its extreme anisotropy. Briefly, Klemens assumes that the thermal waves are strictly longitudinal and transverse (in contradiction to the work of J. Krumhansl)[4] and then by a semi-quantitative analysis concludes that the specific-heat contribution of the longitudinal waves will show a T^3 dependence at a higher temperature than that of the transverse. Although the longitudinal waves will not contribute appreciably to the specific heat because of their high Debye temperature, it is argued that they will be important for the thermal conductivity because the effective relaxation length for the longitudinal modes will be the long crystallite dimension while that for the transverse modes will be the small dimension. Since, furthermore, the longitudinal group velocity will be higher, the total heat conductivity will be weighted much more heavily toward the longitudinal mode than will the specific heat; and if the longitudinal specific heat varies as T^3, the total heat conductivity will tend toward a T^3 dependence also. A disturbing factor about this result is that it does not appear to check quantitatively the existing experimental data. It effectively tries to fit the measurements by an expression of the form $(AT^2 + BT^3)$, which would tend to act like T^2 at lower temperatures unless B/A were great enough over the temperature range considered (say 15 to 50° K) to mask this effect. The result, after fitting the SA-25 data and giving this analysis the benefit of every possible doubt, is that the ratio of the crystallite dimensions must be at least 20:1. This ratio is known to be close to 2:1 for SA-25. From a theoretical standpoint the division of the graphite modes into longitudinal and transverse components is much more artificial than the division into in-plane and out-of-plane components, and furthermore there is some doubt as to whether the former is even possible. A further investigation of this point by group-theoretical methods is presently being undertaken.

B. Thermal Conductivity of Brom-Graphite Residue Compounds - A. Smith, V. Martin

The thermal conductivity and the electrical resistivity of several brom-graphite residue compounds have been measured between 10° and 300° K. The measurements were made on a "self-heating" method apparatus used previously in this laboratory.[5] The samples were prepared for us by G. Hennig[6] at the Argonne National Laboratory.

The thermal conductivity curves of four of these samples are shown in Fig. 2, which also includes curves for an untreated sample and for two neutron-irradiated samples. It can be seen that the slope of the curves decreases as the absolute magnitude decreases. In fact the maximum slope changes from 2.6 for the untreated samples to 2.0 for the 1.16 atom per cent sample. A slope just over 2.0 is also noted for the 12.5 mwd/ct neutron-irradiated sample. On this plot the slope gives the power of the temperature dependence. Since the samples were not measured before treatment, there is a scatter of the order of 10 per cent in the absolute magnitude of the change produced by treatment. The relative values for a given sample as a function of temperature are much more accurate. The curves in Fig. 2 were normalized at 10° K in order that they would not cross.

The electrical resistivity of the same samples is given in Fig. 3. The results show the same trend of reduced temperature dependence with bromination observed by Hennig above 78° K. One striking fact is the tendency of these curves to be quite flat at the lowest temperatures. No explanation is offered for this result. The electrical resistivities of the 30 brominated samples were also measured at room temperature and agree with the results obtained by Hennig.

The thermal conductivity of the brom-graphites was measured to test the possibility that the thermal conductivity of neutron irradiated samples is limited by the scattering of thermal waves by electrons. In the brom-graphites the scattering by the added impurity atoms or ions should be much less than the scattering by defects resulting from neutron irradiation of graphite samples. The bromine atoms are believed to be located at faults and boundaries which are already good scatterers,[6] and thus such atoms should not decrease the

619-12

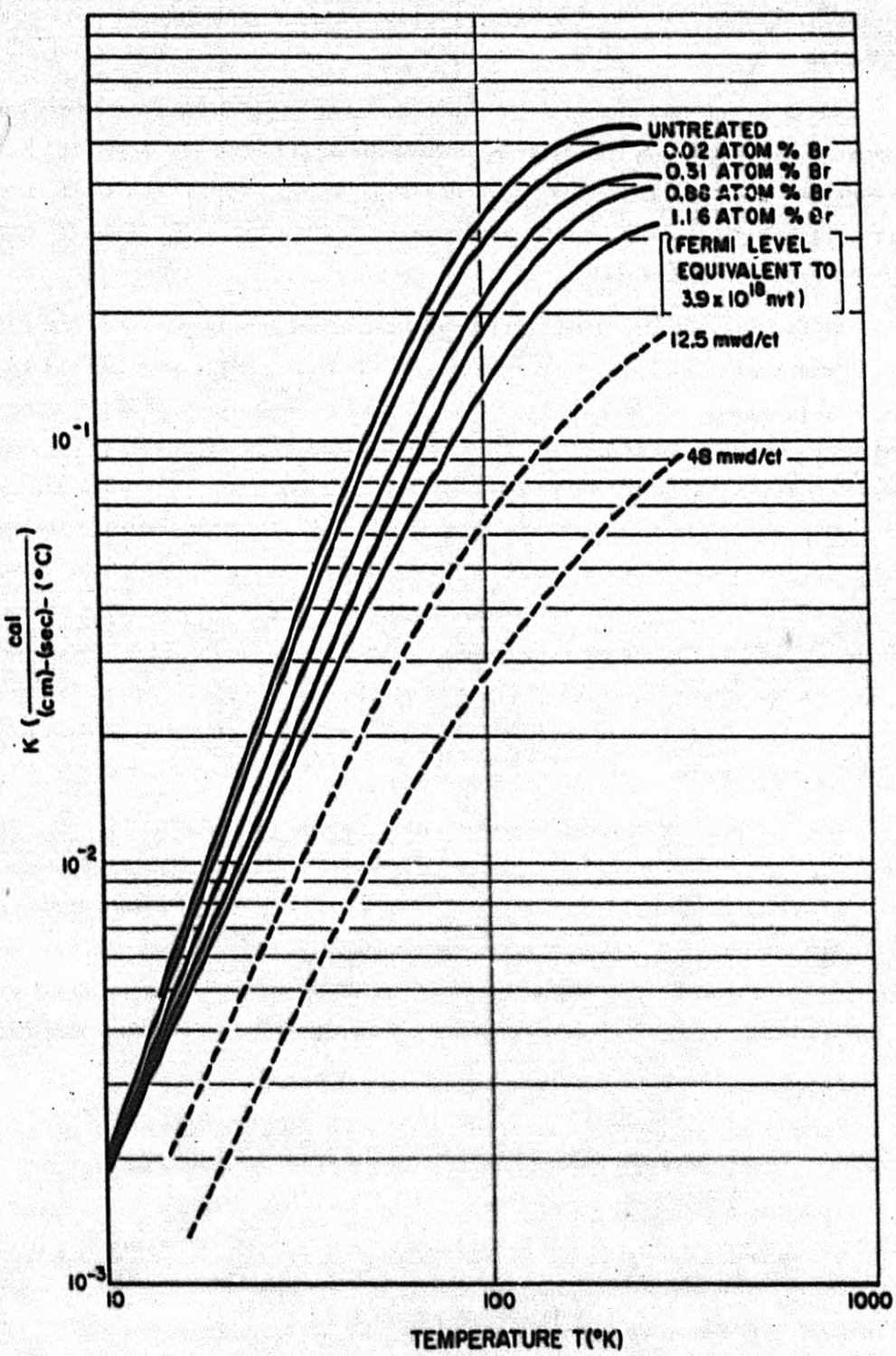

Fig. 2. Thermal Conductivity of Neutron Irradiated and Brominated AGOT-KC Graphite

619-12

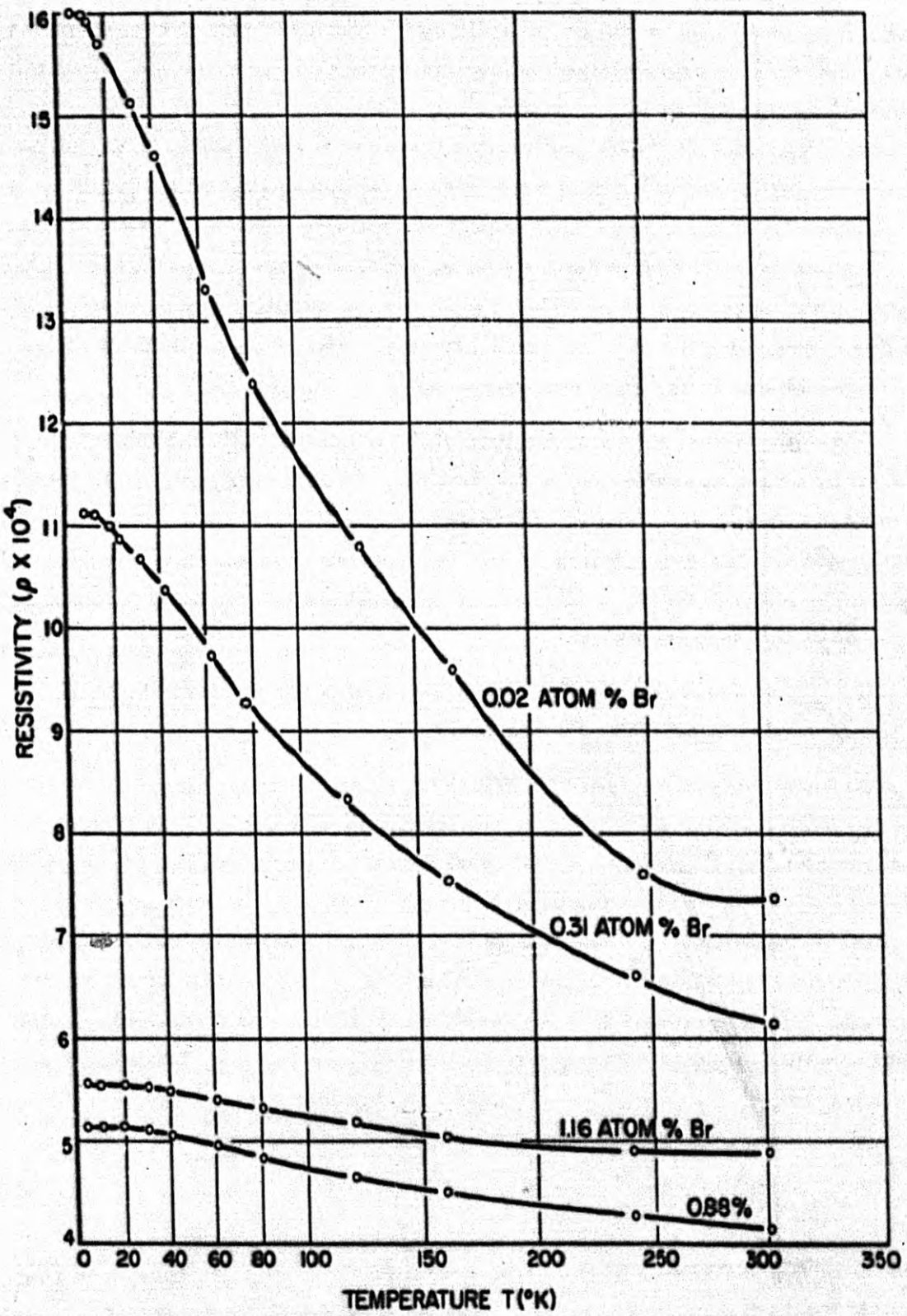

Fig. 3. Resistivity of Brom-Graphite vs Temperature

619-14

mean-free path. On the basis of Hall-coefficient and magnetic-susceptibility measurements a correlation of equivalent change in electron concentration caused by bromination and that caused by neutron irradiation has been derived.[7] For the units used here the correlation factor is 1 atom per cent Br equivalent to 20 mwd/ct in a Hanford test hole. It can be shown that on the basis of the curves in Fig. 2 the change in thermal conductivity caused by bromination is at most one third of that caused by the equivalent neutron irradiation. This result is interpreted to mean that the thermal conductivity of neutron-irradiated samples is not limited by electron scattering. The neutron-induced changes must then be due to the imperfections caused by the irradiation.

The question of whether the thermal conductivity of the brom-graphites is limited by electron scattering is not settled. To test this point, however, similar measurements will be made on bisulfate-graphite compounds. An equivalence with the brom-graphites should be obtained if electron scattering is important, and if not the results should differ since the bisulfate radical is larger than the bromine atom.

C. Field Dependence of the Hall Coefficient and Magneto Resistance of Irradiated Graphite - J. D. McClelland

The field dependence of the Hall coefficient and the magneto resistivity have been determined at fields ranging from 5 to 15 kilogauss for a series of irradiated artificial graphite samples with exposures up to 12 mwd/ct (Hanford Works cooled B test hole equivalent). Figure 4 shows the variation of the Hall potential in millivolts as a function of field. In all cases the Hall potential is seen to increase linearly with the field and extrapolate to zero at zero field as expected. The magneto-resistivity coefficient on the other hand changes its behavior with exposure. The relation which defines the magneto-resistivity coefficient is

$$\frac{\Delta R}{R} = AH^{\gamma}$$

where R is the resistance of the sample at zero field, ΔR the change in resistance due to the applied magnetic field H, A is the magneto-resistivity coefficient, and γ is a constant. By plotting $\frac{\Delta R}{R}$ as a function of field strength on a log-log plot as shown in Fig. 5, it is possible to determine the exponent

619-15

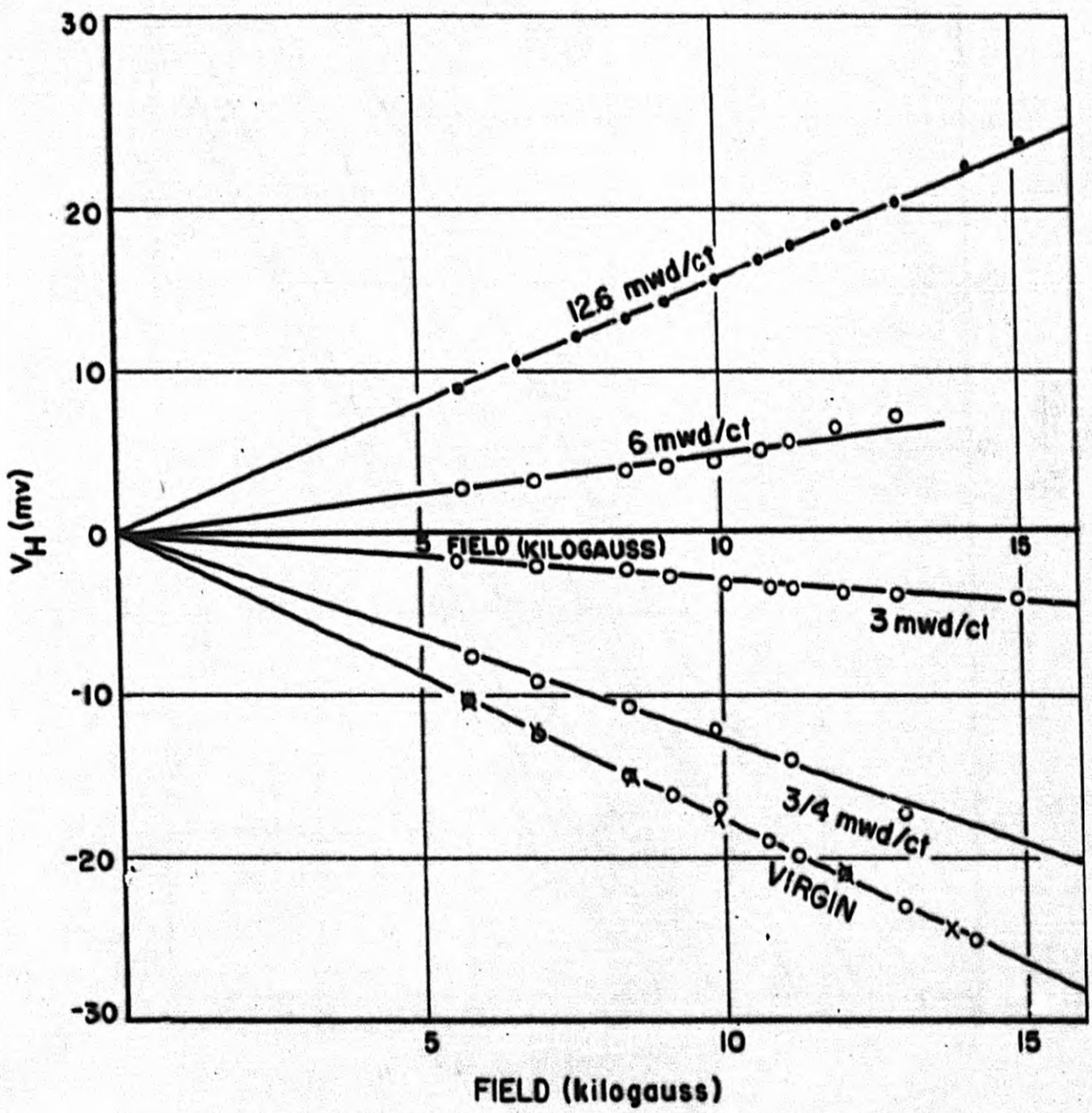

Fig. 4. Variation of the Hall Potential with Field Strength

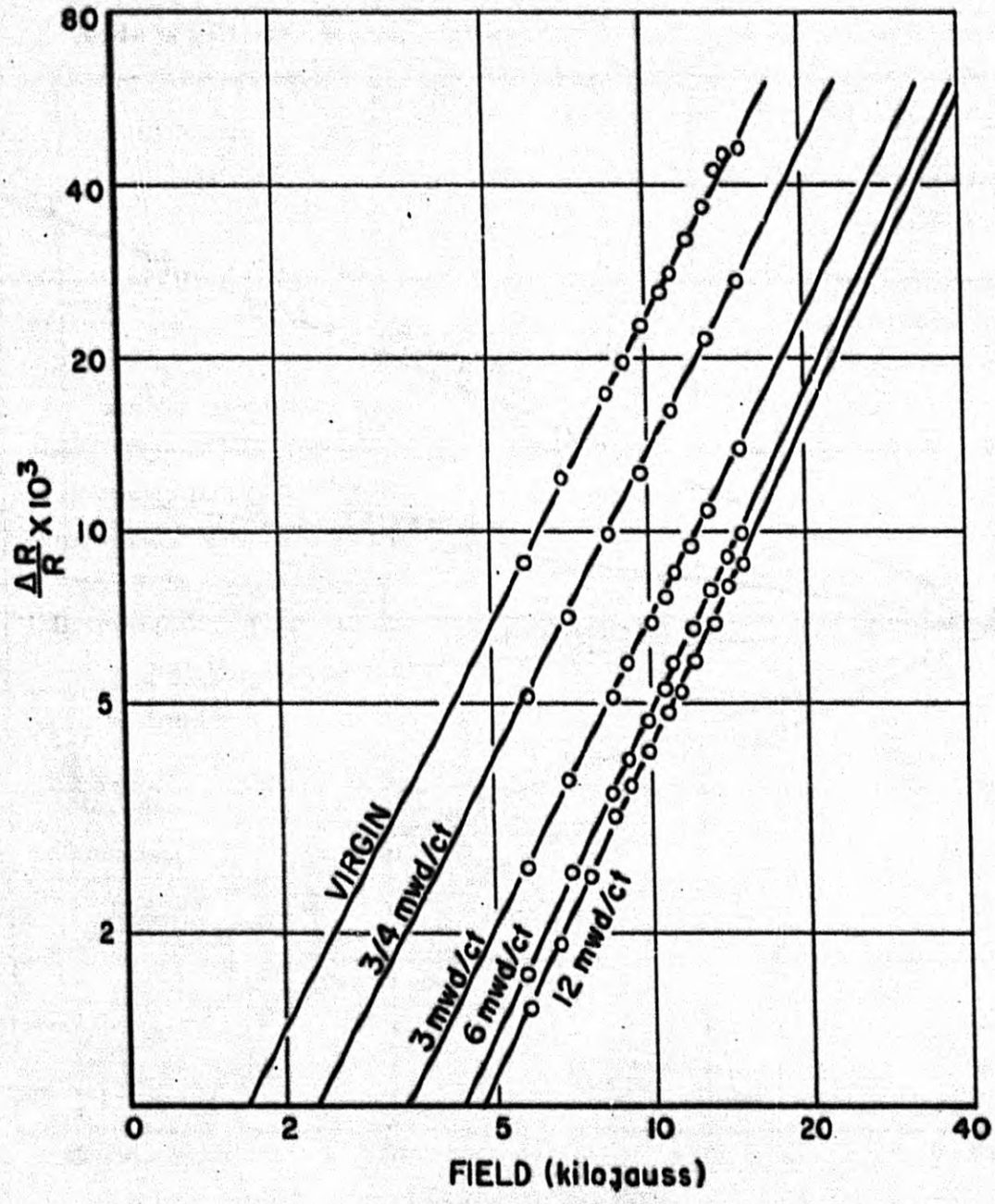

Fig. 5. Variation of the Magneto-Resistance of Graphite with Field Strength

619-17

γ for the various samples. Figure 6 shows the variation of this exponent with exposure. A precision of $\pm$ 0.002 is assigned to these values. The value for the exponent apparently increases linearly with exposure, starting at about 1.77 for the virgin material and attaining a value of 1.88 for the 12.6 mwd sample.

D. Cyclotron Irradiation of Graphite - W. S. Gilbert, D. L. Clark, J. H. Pepper

Nine cyclotron irradiations of graphite targets at temperatures of -170°, 25°, and +150° C have been made during this period. These have been directed at elucidating the nature of the processes responsible for annealing of radiation damage in the low-temperature region and to determine if the rate of this annealing is affected by the presence of the damaging radiation. Targets from six of the runs are in Downey undergoing measurements of thermal conductivity, thermoelectric power, electrical resistivity as a function of temperature, and also of stored energy as a function of low-temperature annealing. In the remaining three of the runs, in-place measurements of thermoelectric power (Q) and electrical resistivity (ρ) were made at intervals during irradiation with 10 Mev protons. These runs were the following:

Run Designation	Irradiation Temperature °C	Target Thickness (inches)	Maximum Exposure (μah/cm^2)
C-365*	-170	0.010	40
C-375	-170	0.004	14
C-368	25	0.005	18.1

*Run C-365 was reported in NAA-SR-909[8] in a preliminary form.

The curves obtained for the properties as a function of temperature after various irradiations at 25° C (C-368) are shown in Figs. 7 and 8. The data compare favorably with results obtained in an earlier similar run (C-363) reported previously [9]

In Figs. 9 and 10 the values of Q and ρ measured at -190° C are compared for irradiations made at 25° C and at -170° C and for subsequent annealing at room temperature of one of the -170° C samples. It is seen that fair agreement

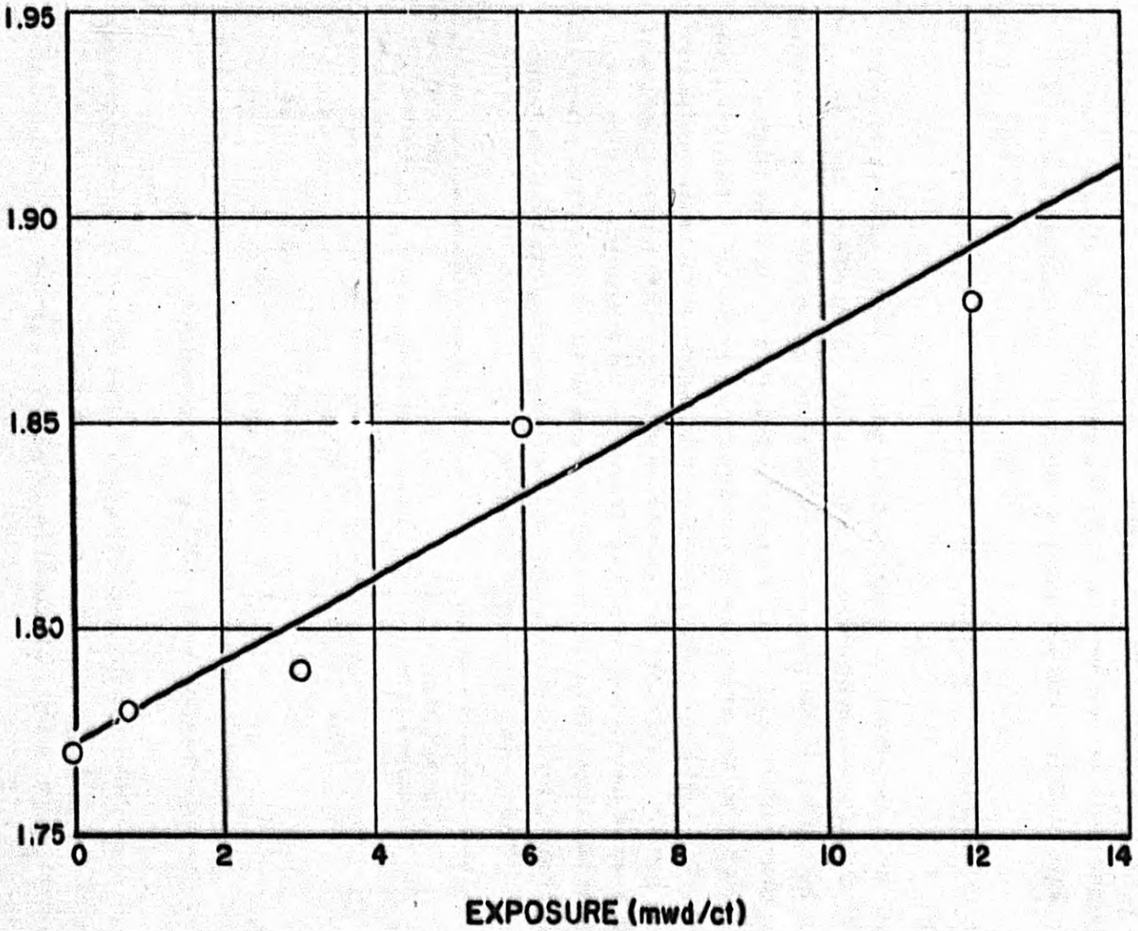

Fig. 6. Variation of the Exponent γ ($\Delta R/R = AH^{\gamma}$) with Exposure

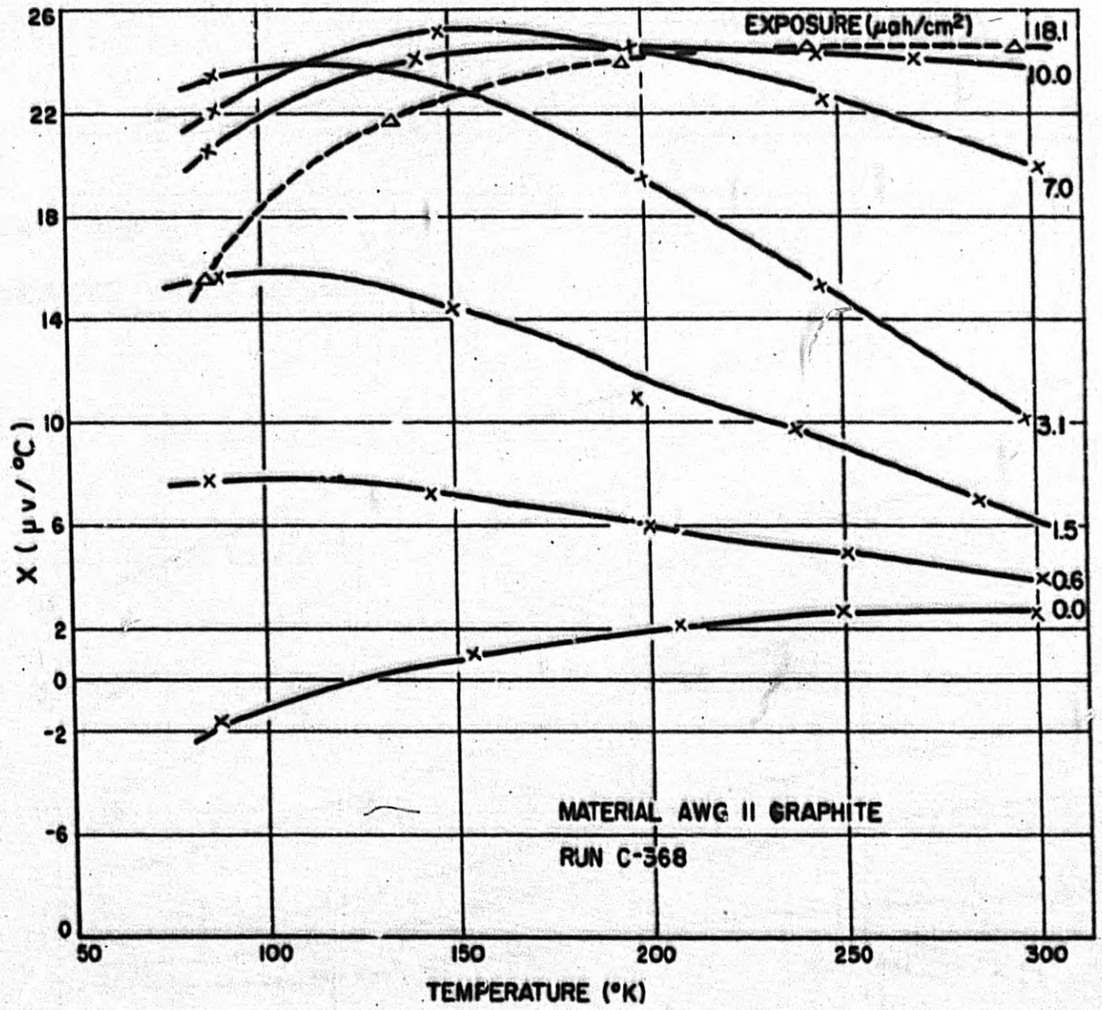

Fig. 7. Thermoelectric Power Relative to Lead at Low Temperatures for Increasing Amounts of Irradiation at 25° C with 10-Mev Protons

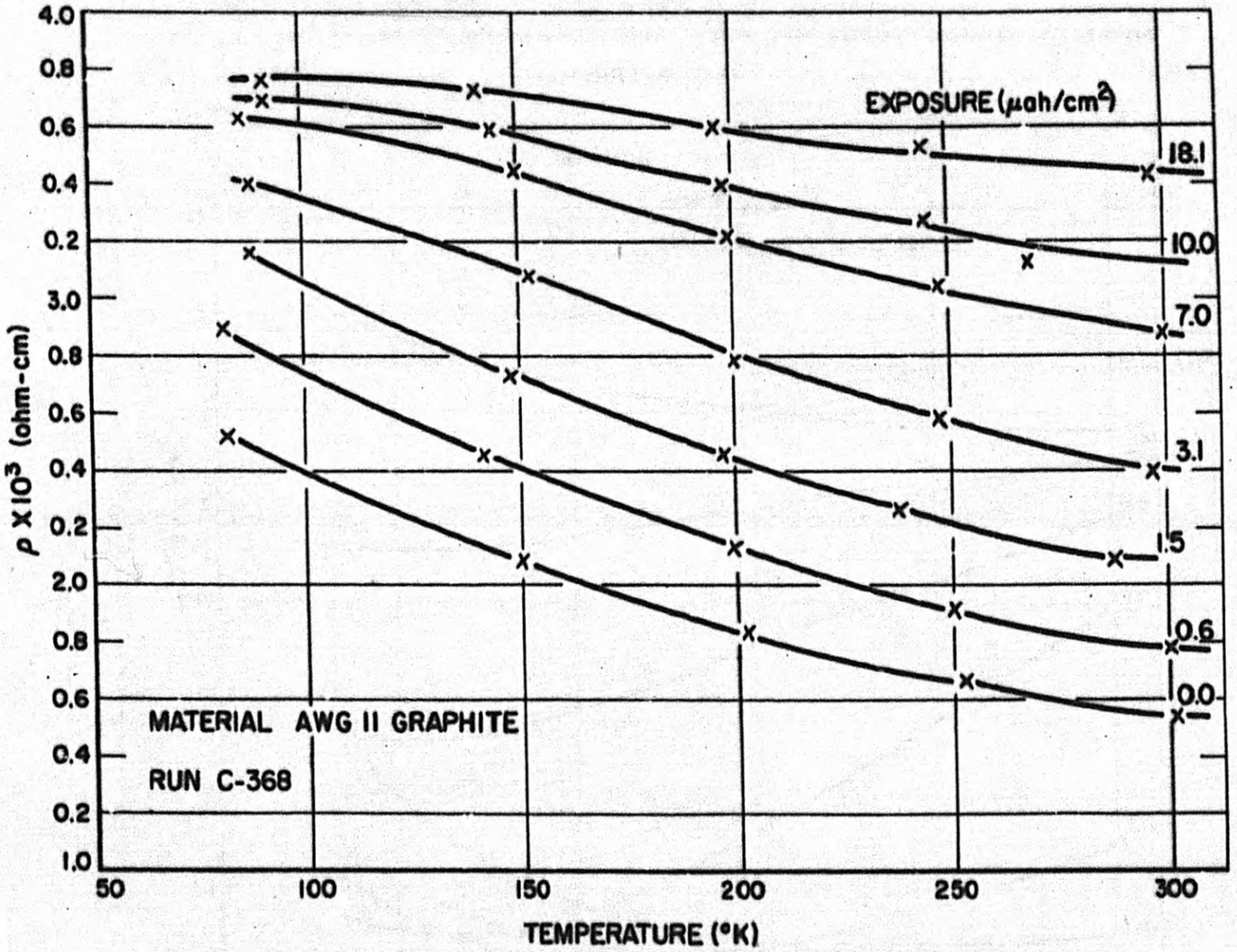

Fig. 8. Electrical Resistance at Low Temperatures for Increasing Amounts of Irradiation at 25° C with 10-Mev Protons

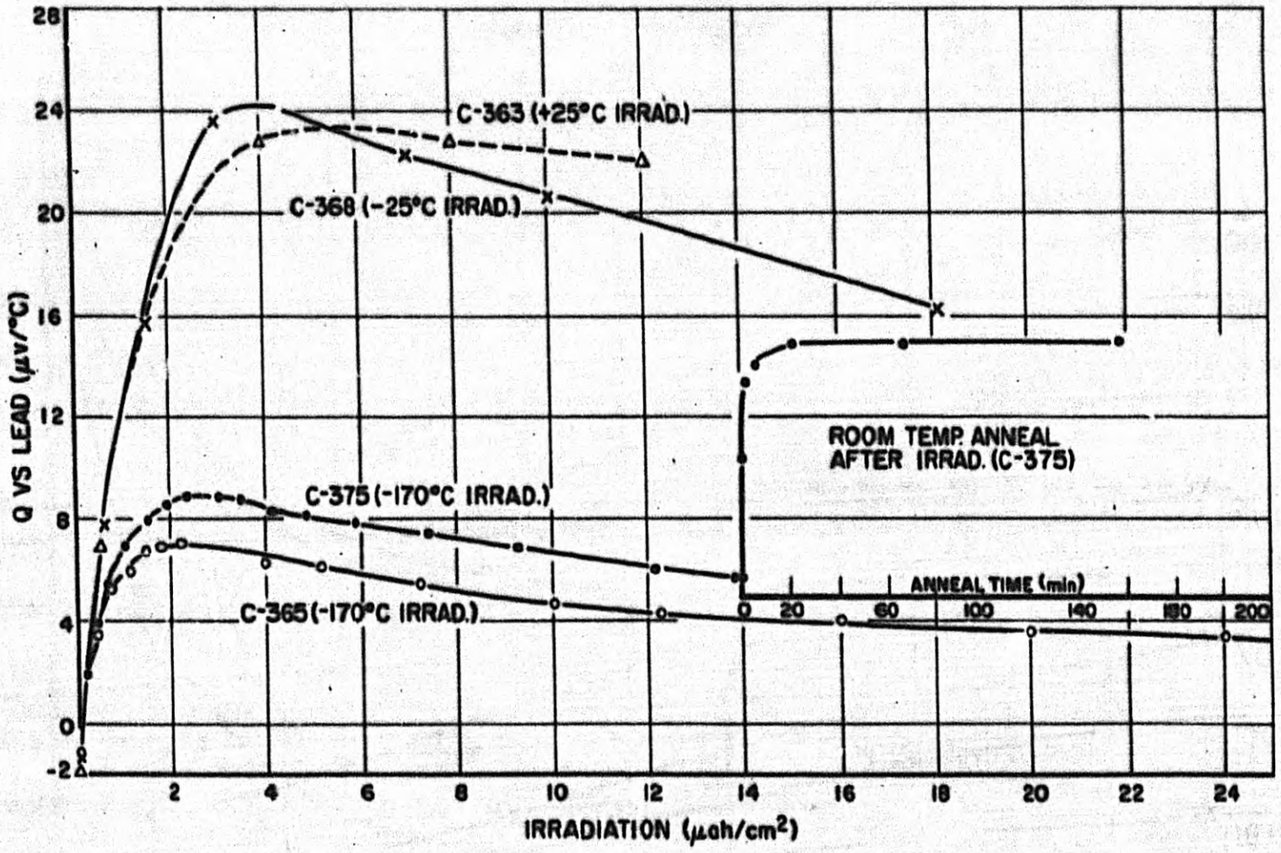

Fig. 9. Thermoelectric Power Relative to Lead Measured at -185° C as Function of Irradiation for Room Temperature Irradiation and for Low Temperature Irradiation Followed by Thermal Annealing at Room Temperature

619-22

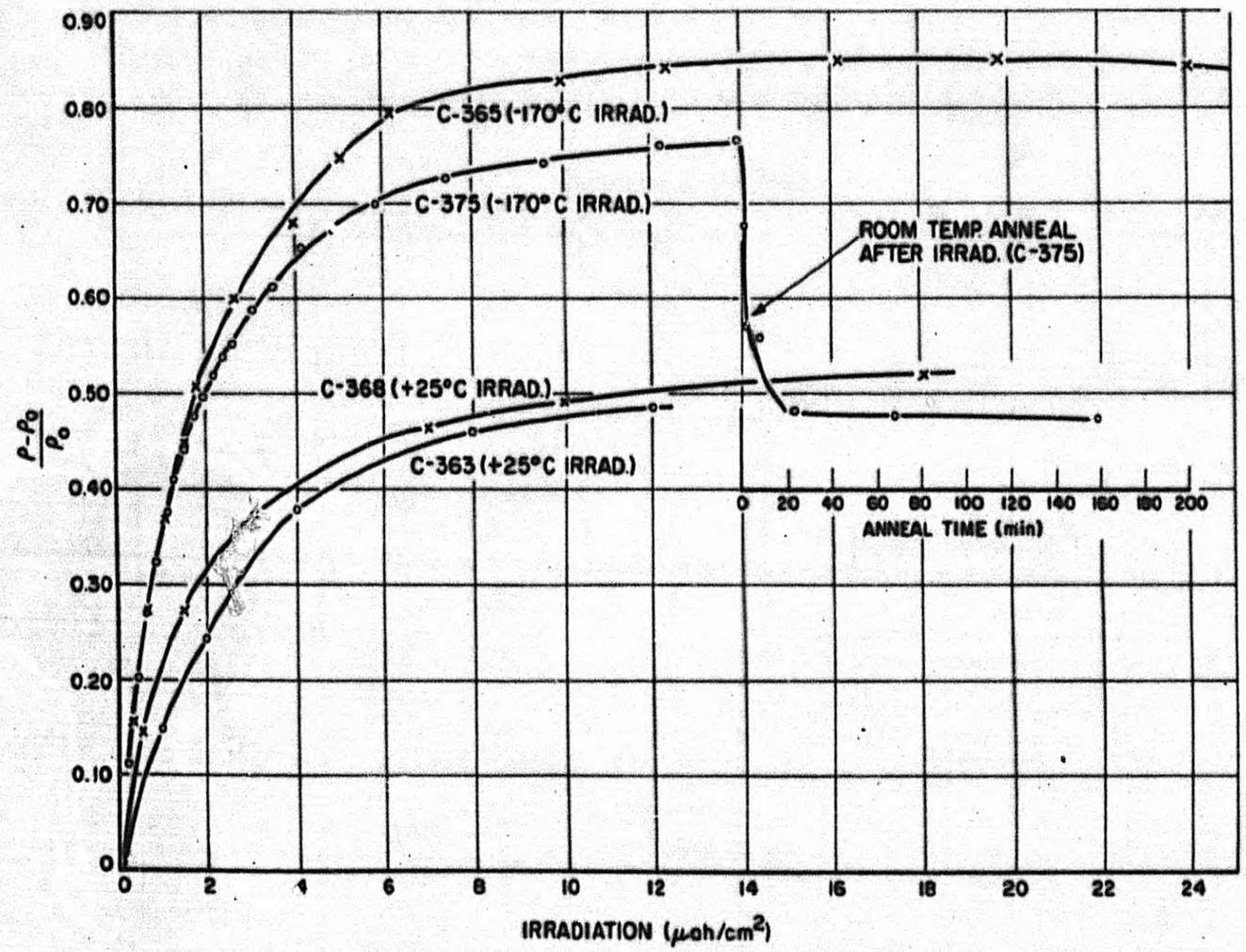

Fig. 10. Fractional Change Electrical Resistivity Measured at -185° C as Function of Irradiation and for Low Temperature Irradiation Followed by Thermal Annealing at Room Temperature

9417-1013

between the two -170° C samples is obtained, and that the sample annealed to room temperature reaches approximately the value achieved by the 25° C irradiated samples. The maximum attained by the thermoelectric power is significantly different for the two different temperatures of irradiation.

E. Asymptotic Aging Experiments - R. L. Carter

The measurements of the release of stored energy during quasi-isothermal annealing in a constant temperature oven at temperatures from 100 to 300° C reported previously[10, 11] have been continued. In the former reports the annealing was described in terms of a predominant annealing process of the third order. In addition, two processes of the first order were invoked to account for the remaining energy release. The third order process is adequate to account for the characteristic long tail in the Sykes' annealing curve which has led in the past to postulation of annealing processes of even higher order.[12] In addition to the inherent improbability of a process of the third order the most disturbing feature of the results of the earlier analyses was the large fluctuation with degree of irradiation in calculated values of the coefficient $\nu \exp(-A/kT)$ in the rate equation

$$-\frac{dn}{dt} = \left[\nu \exp(-A/kT)\right] n^3 .$$

The data have been re-examined in the light of the assumption of simultaneous processes of the first order. The experimental data obtained during each individual run were divided into two regions: those obtained during the early part of the run, when the temperature divergence is large, and those obtained during the latter part, when the sample temperature is approaching oven temperature. In the latter region when

$$\frac{A_i}{k} \ll \frac{T_o^2}{T - T_o} ,$$

the data may be regarded as isothermal. The rate of release of energy may be described as

$$-L' = \Sigma_i (-L_i') = \Sigma_i \left[\nu_i \exp(-A_i/kT_o)\right] L_i ,$$

where L is the total stored energy; L_i is the amount of energy "stored" in process "i"; L' and L_i' are their time derivatives; ν_i is the rate factor of process "i"; A_i is the activation energy of process "i"; and T_o is the final temperature which the specimen temperature T, is approaching.

The values of $\ell n(-L')$ in the isothermal region have been plotted vs time of anneal t. It is found that in every case the resulting semi-log plot is a curve which can be resolved, in the same manner as a radioactive decay curve, into a set of straight lines corresponding to component exponential decays of periods $1/\nu_i \exp(-A_i/kT_o)$. In nearly all cases two such components result in an excellent fit of the experimental data over the quasi-isothermal region of the data (see Fig. 11).

The slope of each of the straight lines in the annealing plot is regarded as corresponding value of the rate factor, $\nu \exp(-A/kT_o)$, for the process, while the quotient $(-L')/\nu \exp(-A/kT_o)$ formed at any point on one of the lines is the apparent stored energy remaining to be released through the process.

The non-isothermal portion of the data is analyzed in an entirely different manner. In regions of large temperature change, a single first-order process may be described by

$$\ell n_e(-L'_a/L_a) = -(A_a/k)(1/T) + \ell n_e \nu_a$$

so that a plot of $\ell n_e(-L'_a/L_a)$ vs $(1/T)$ will yield a straight line of slope $(-A_a/k)$ as long as one process alone is primarily operative. The value of $(-L'_a/L_a)$ at the point where T passes through T_o is the value of the rate factor $\nu \exp(-A_a/kT_o)$ for the process. The values of L_a used in forming the ratios must be obtained through intergration of L'_a,

$$L_a = L_o - \int (-L'_a)dt \quad .$$

An appropriate value of the initial energy, L_o, to be released through this process must be estimated. In Fig. 12 representative data are plotted for various choices of L_o. The value of activation energy determined from the slope of the curves is seen to be insensitive to the choice of L_o. The character of the curve, however, is quite sensitive to a choice of L_o, as is the value of

619-25

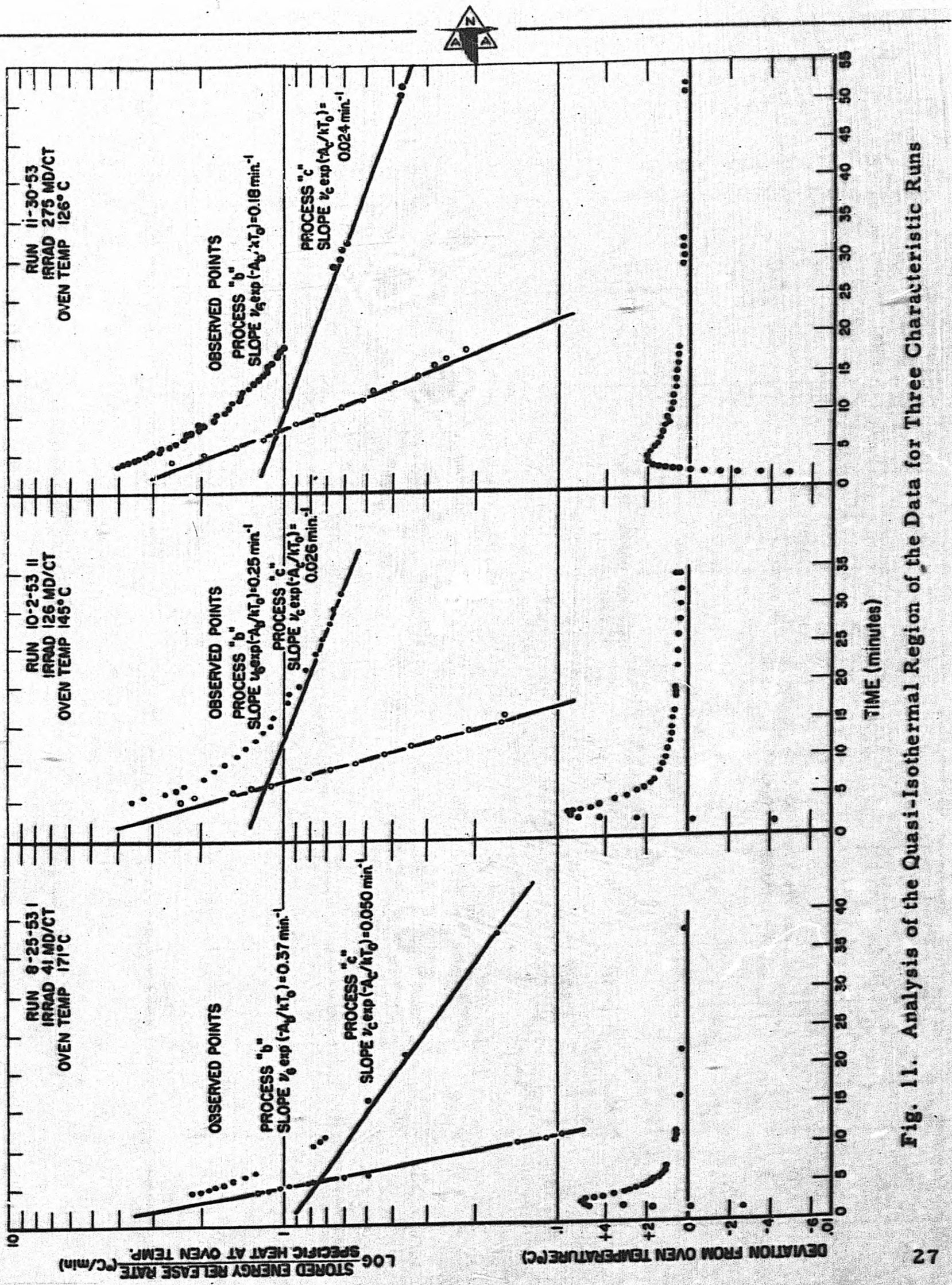

Fig. 11. Analysis of the Quasi-Isothermal Region of the Data for Three Characteristic Runs

619-26

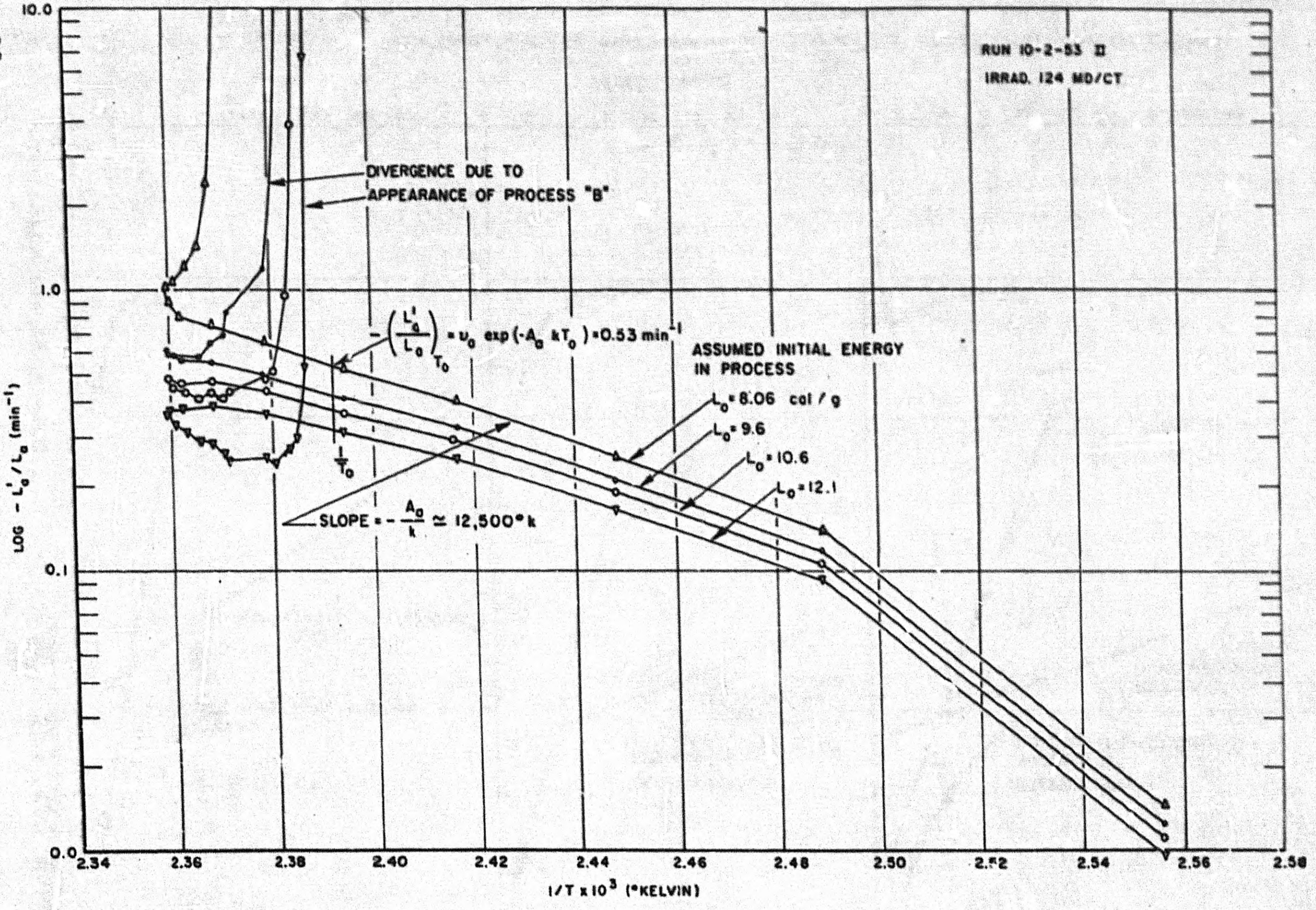

Fig. 12. Plots of Log $(-L'/L)$ vs $1/T$ for Various Choices of L_o

the rate factor determined from the curve. A choice of L_0 is made which causes the points to be along the nearest approach to a straight line. The later departure of the points from the linear curve in the positive direction of $\frac{-L'}{L}$ is assigned to the emergence of other processes leading to excess rate of energy release.

A tabulation of data obtained by this analysis is given in Table I. It is noted that the differing rate factors establish that the process observed during the temperature rise is generally different from the processes observed during the quasi-isothermal portion of the run. In Fig. 13 the logarithm of the rate factors for all runs is plotted vs $1/T_0$ in an analogue of the curve of Fig. 12 for a single run. A coherent general trend is evident in which the activation energies determined within the individual runs (slopes of lines three points) are seen to be consistent with the activation energies obtained by comparing rate constants between runs made at different temperatures.

The columns labeled L_b and L_c in Table I are the minimum values of the initial energy to be released through the processes observed in the quasi-isothermal portion of the run. These values are obtained by extrapolation of each of the component straight lines of Fig. 11 back to the time when the sample temperature passed through T_0. If the processes are independent, the actual rates of energy release must surely be greater during the temperature overshoot than calculated by assuming isothermal annealing during this interval of time. Hence the assumed initial energy content obtained by evaluating $\left[-L'/\nu \exp(-A/kT_0)\right]$ at this point must constitute a lower limit under the assumption of independence. However, when the sum $L_0 + \sum L_i$ is formed and reduced by the amount apparently remaining in the process remaining operative at the termination of the experiment, it is found to exceed by a substantial amount the total energy actually observed to be released (see last column, Table I). This result clearly indicates that the assumption of independence of the processes is not correct; i.e., that the processes observed during the quasi-isothermal portion of the anneal are not independently operative during the rising temperature portion of the anneal.

619-28

TABLE I

SUMMARY OF QUASI-ISOTHERMAL STORED ENERGY DATA

Run	Irradiation (cal/g-hr)	Annealing Temperature T_a (°K)	Temperature Equivalent ΔT_{equiv}	Total Energy Released at Temperature $\beta(1-\alpha/3\alpha)$ (cal/g)	Total Apparent Energy Content at Temperature H_{T_a} (cal/g)	Quasi-Isothermal Region: Activation Energy E_a/R (°K)	Quasi-Isothermal Region: Rate Factor $\left(\frac{d\alpha}{dt}\right)_0$ (sec^{-1})	Quasi-Isothermal Region: Initial Energy h_i (cal/g)	Quasi-Isothermal Region: Rate Factor $\left(\frac{d\alpha}{dt}\right)_0$ (sec^{-1})	Quasi-Isothermal Region: Maximum Initial Energy h_i (cal/g)	Quasi-Isothermal Region: Rate Factor $\left(\frac{d\alpha}{dt}\right)_0$ (sec^{-1})	Quasi-Isothermal Region: Maximum Initial Energy h_i (cal/g)	Quasi-Isothermal Region: Residual Energy h_r (cal/g)	Difference $h_a + \Delta h_a - h_r - \beta(1-\alpha/3\alpha)$ (cal/g)
5-26-53	12.5	478	6.97	6.37	6.39	7400	1.12	1.4	1.38	0.68	0.007	0.81	0.017	0.13
									0.31	0.721				
7-17-53	12.3	486	6.81	6.66	6.66	40000	0.52	1.1	0.93	0.32	0.021	1.7	0.4	1.8
									0.23	1.31				
7-22-53	60	484	6.23	13.4	13.7	33700	~1	-	0.27	3.2	0.007	3.9	0.96	3.9
						30000	0.63	15.1***						
7-27-53	166	662	14.4	24.2	25.1	11500	0.33	14.7	0.29	4.8	0.004	18.9	1.3	6.9
7-28-53	400	662	24.7	34.2	35.4	11000	0.84	21	0.12	6.4	0.022	12.4	2.2	3.4
7-30-53	2304	662	3.2	13.7	13.9	11400	0.44	1.7	0.35	3.0	0.001	7.5	1.2	6.3
8-21-53	92	664	17.1	28.4	25.0	12500	1.3	10	0.22	2.8	0.004	7.2	2.2	-0
8-24-53	5 $\frac{watts}{cm^2}$	660	6.99	8.68	8.94	12100	1.3	1.4	1.8	0.50	0.31	1.8	0.19	1.1
8-25-53 I	61	664	3.2	13.9	14.8	8400	1.3	5.1	0.37	2.5	0.050	5.3	0.89	2.1
8-25-53 II	116	664	21.6	25.9	26.9	14000	1.3	-	0.14	2.7	0.02	11	5	1.3
						7500	1.31	15.0***						
10-1-53	278	664	129	33	83	8700	0.21	82.5	-	-	-	-	-	-
10-2-53 I	278	618	11.6	26.7	21.9	11000	0.43	15.1	-	-	0.049	7.7	1.2	6.9
10-2-53 II	116	618	5.06	16.7	22.3	12500	0.53	5.6	0.23	3.9	0.026	12.8	5.6	6.8
10-2-53 III	92	614	4.31	16.5	15.6	6900+	0.34	5.8	0.11	0.0	0.023	12.5	3.1	9.8
11-27-53 I	12.8	614	0.29	1.3	1.48	8000+	0.6	0.7	0.69	0.07	0.007	0.91	0.097	10
11-27-53 II	12.7	614.3	2.39	5.1	6.7	28000+	0.23	1	0.12	1.6	0.012	3.6	2.5	1.5
11-27-53 III	48	614.3	2.10	6.63	5.35	19000+	0.23	1.9	0.38	1.22	0.044	3.5	0.52	1.2
11-27-53 IV	12.8	608	0.49	0.63	1.15	-	-	-	0.17	0.27	0.03	0.61	0.32	-
11-30-53	275	399	5.1	14.3	11.9	17500	0.15	7.7	0.18	6.6	0.026	12.1	3.6	1.9
12-1-53 I	61	399.3	6.76	5.2	6.25	47000	~0.2	~3.5	0.35	0.67	0.060	3.8	1.04	1.5
						18000+	0.13	3.9***						
12-1-53 III	460	395.7	0.76	6.65	11.23	40000	~0.1	~4.5	0.14	7.5	0.03	6.4	6.4	0.6
						23000	0.57	5.0***						
12-2-53 I	146	395.3	0.31	3.65	6.25	38000+	0.10	2.4	0.099	1.6	0.015	6.9	2.6	3.1
12-2-53 II	1534	395.3	0.023	0.49	0.49	300000(?)	2(?)	0.12(?)	0.11(?)	0.19(?)	-	-	-	-
2-12-54	460	423.3	5.4	27.6	46.6	10640	0.34	12.9	0.30	5.2	0.017	33.5	10.8	8
2-13-54 I	208	428.3	11.9	24.6	29.4	12100	0.64	11	0.16	4.5	0.026	12.5	6.8	2.6
2-13-54 II	126	428.3	7.4	19.2	22.3	11400	0.66	11	0.16	4.1	0.028	9.6	3.1	2.4
2-14-54 I	92	428.3	6.5	15.2	18.3	13400	0.64	2.7	0.17	5.1	0.027	9.8	3.1	0
2-14-54 II	41	428.3	2.3	7.7	9.2	12100	0.62	5.2	0.33	2.4	0.054	6.4	1.5	3.0
2-17-54	275	429	9.2	27	31.6	10000	0.95	14	0.13	6.6	0.019	13.4	4.8	2.2
2-22-54	650	428	7.9	23.8	33.8	17700	0.64	~60	0.23	7.6	0.021	21.7	12	~30
3-13-54	48	406	0.54	27.4	27.5	>4000	>0.65	~27	1.0	6.0	0.24	1.4	0.12	6.8

* Cyclotron irradiation with alpha particles
† Three processes apparent in Quasi-Isothermal Region
**Two slopes apparent in ln L'/L vs $\frac{1}{T_a}$ plot

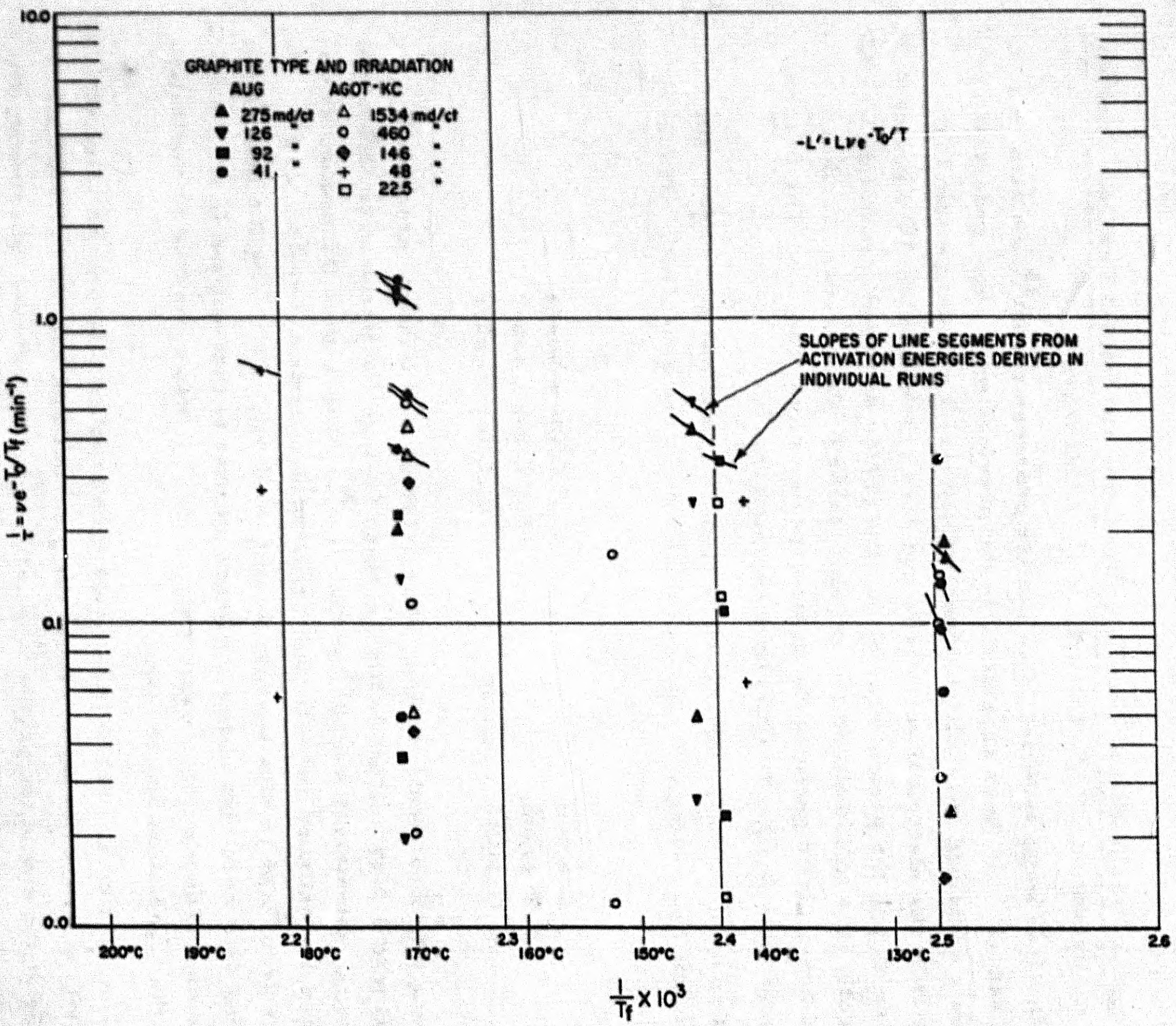

Fig. 13. Rate Factors $\nu_i \exp(-A_i/kT_o)$ of the Processes in Various Runs as a Function of $1/T_o$ (Reciprocal of the Absolute Temperature of the Oven)

II. METALS

A. Cyclotron Irradiation of Thorium, Uranium, and Gold-3 Per Cent Thorium

J. A. Brinkman, W. S. Gilbert and C. J. Meechan

An experiment reported in an earlier progress report[13] and also in a topical report[14] has been repeated. In the previous work some uncertainties in the data remained unresolved. Specifically, (1) it was not certain that saturation of the electrical resistivity had been reached in the Au-3 per cent Th specimen during the proton irradiation, and (2) the deuteron irradiation was not sufficiently long to determine the ultimate shape of the curves. Further, it seemed desirable to perform the same experiment on uranium. The present experiment was designed to clarify these matters.

Two uranium foils, one Ames thorium foil, and one gold-3 per cent thorium foil, all having a 0.002-inch thickness, were annealed in vacuum as follows:

Uranium	600° C for 2 hours
Thorium	600° C for 2 hours
Gold-3% Thorium	300° C for 2 hours

Following this treatment, the foils were irradiated at temperatures below -140° C with 9-Mev protons in the Berkeley 60-inch Cyclotron to an integrated flux of approximately 3.4×10^{18} protons/cm^2. At this point the proton irradiation was discontinued and a further irradiation of approximately 2×10^{18} deuterons/cm^2, of 18 Mev energy, was carried out. Following the irradiation annealing data were obtained in a manner similar to that utilized in the previous experiment. The electrical resistivity at -180° C was measured periodically during the irradiation and annealing.

The thorium and uranium samples each reached a saturation value of resistivity whereas the resistivity of the gold-thorium sample was still increasing at the end of the proton irradiation. In the previous experiment, the resistivity increase for the gold-thorium specimen was 69 per cent; whereas in the present work an increase of 87 per cent was obtained. In the earlier

619-81

work an increase in resistivity was observed when the deuteron irradiation was started, while a decrease was found in the present experiment. The discrepancy here is ascribed to the failure to reach saturation with the proton irradiation in the earlier work. Perhaps the decrease observed in the present experiment would have been even more pronounced if complete saturation had been reached during the proton irradiation.

It is interesting to compare the saturation values of the pure thorium and uranium samples. The initial slopes of the curves are comparable but the uranium saturates at about one fifth the level of the thorium. This difference in saturation values may indicate that the minimum stable interstitial-vacancy separation in uranium is about twice that in thorium.

The initial decrease in resistivity upon deutron irradiation was observed in all three materials studied in the present work. As has previously been explained, this decrease indicates the annealing of interstitial-vacancy pairs by fission fragments. However, the longer deuteron irradiation of the present experiment gave a further effect. This effect was characterized by an increase in resistivity following the initial decrease. A possible mechanism for an increasing tendency in the resistivity has been offered previously.[13,14] This mechanism (the formation of dislocation loops) was erroneously applied to the observed increase in the Au-3 per cent Th specimen upon deuteron irradiation in the earlier work, a result which has been shown to be false by the present experiment. One might expect a longer relaxation time for the formation of dislocation loops than for the process of annealing interstitial-vacancy pairs. Thus a combination of these two processes seems to offer an adequate explanation for the observed shape of the curves, i.e., a sharp decrease followed by a slowly recovering increase.

B. Annealing Studies of Cold-Worked and Irradiated Thorium - C. J. Meechan

An attempt is being made to study various fissionable metals from the standpoint of lattice imperfections. In connection with this work it was decided to look for well-defined annealing states in cold-worked and irradiated thorium by using a method similar to that which enabled the isolation of interstitial and vacancy annealing states in copper.[15] If such states were found, it would then be desirable to obtain activation energies for the particular regions and to try

to interpret the results using the knowledge already obtained for copper. The fact that both metals have the same structure (f. c. c.) is a favorable factor in connection with such an approach.

For the cold-work studies wires of Ames thorium approximately 4 inches long and having a diameter of 0. 020 inch were twisted in liquid helium. Tempering curves were then obtained, a typical curve being that shown in Fig. 14. Measurements on the cold-worked specimens above room temperature have not been made as yet because of probe difficulties.

Similar curves which have been obtained for cyclotron-irradiated thorium are shown in Fig. 15. It is apparent that in both the cold-worked and irradiated specimens a sharp annealing state is prominent in the vicinity of room temperature. In addition the irradiated specimen has another pronounced annealing state in the vicinity of 300° C.

The work is being continued with the emphasis at present on the room-temperature state. Attempts are being made to obtain activation energies for this state from both cold-worked and cyclotron-irradiated specimens.

C. X-ray Diffraction - G. D. Collins

A study of the instrumental broadening of X-ray diffraction lines was completed. It was found that for a Philips High Angle Goniometer the function $(1 + k^2x^2)^{-3/2}$ gives a good representation of the X-ray line shape of an annealed sample. The fourier transform of this function, for a $K\alpha_1$ and $K\alpha_2$ doublet, is of the form

$$\frac{g}{k} K_1 \left(\frac{g}{k}\right) \cdot \left[1 + \zeta \operatorname{cis} (2 \pi x_1 g)\right]$$

where ζ is the ratio of intensities of $K\alpha_2$ to $K\alpha_1$, x_o is the angle of separation of the $K\alpha_1$ and $K\alpha_2$ peaks, and $K_1\left(\frac{g}{k}\right)$ is the Bessel function of the second kind. These results can be used to eliminate the instrumental broadening of a broadened X-ray line when the specimen being studied cannot be annealed as in the case of uranium.

619-33

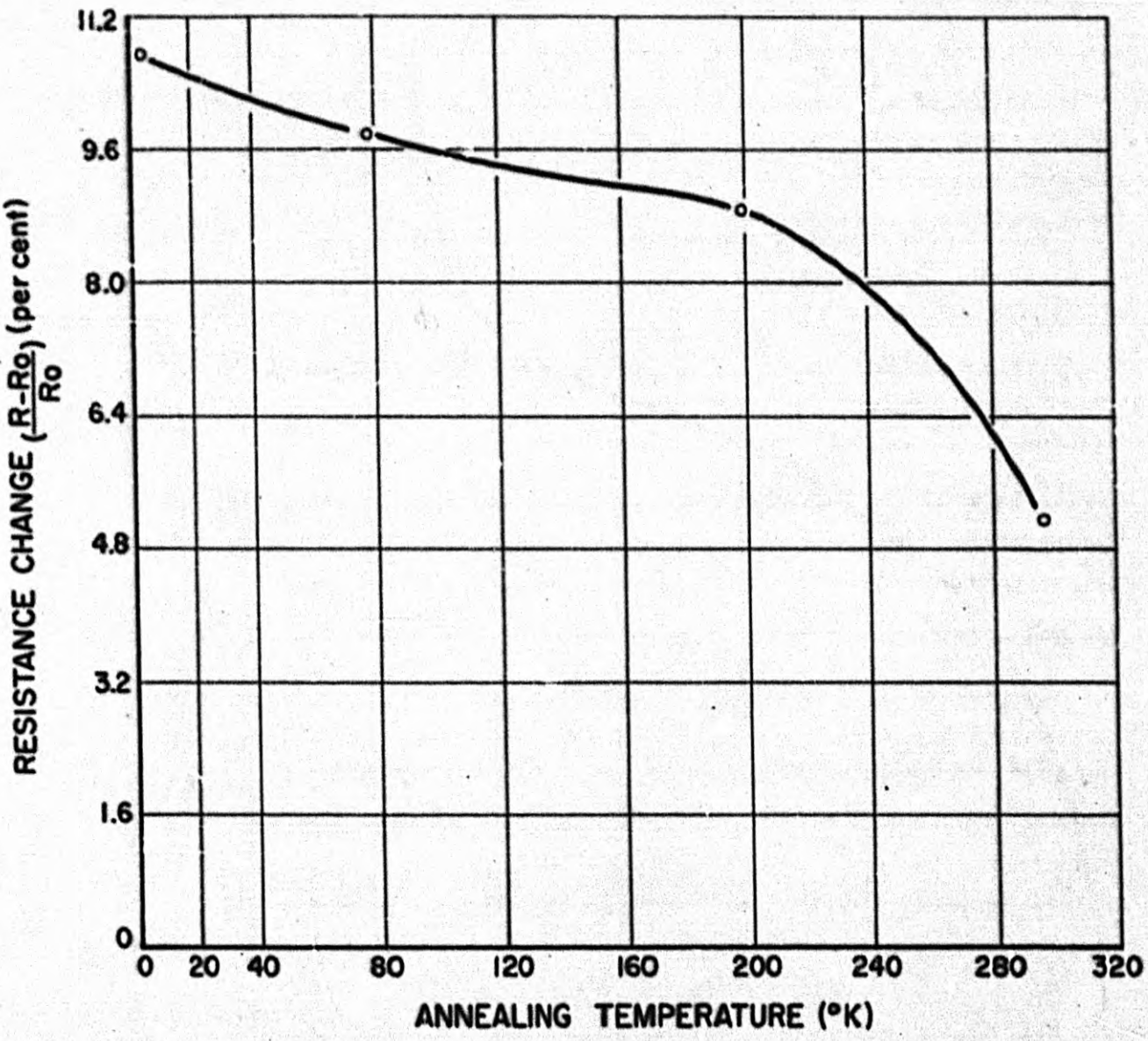

Fig. 14. Tempering Curve for Cold-Worked Thorium

619-34

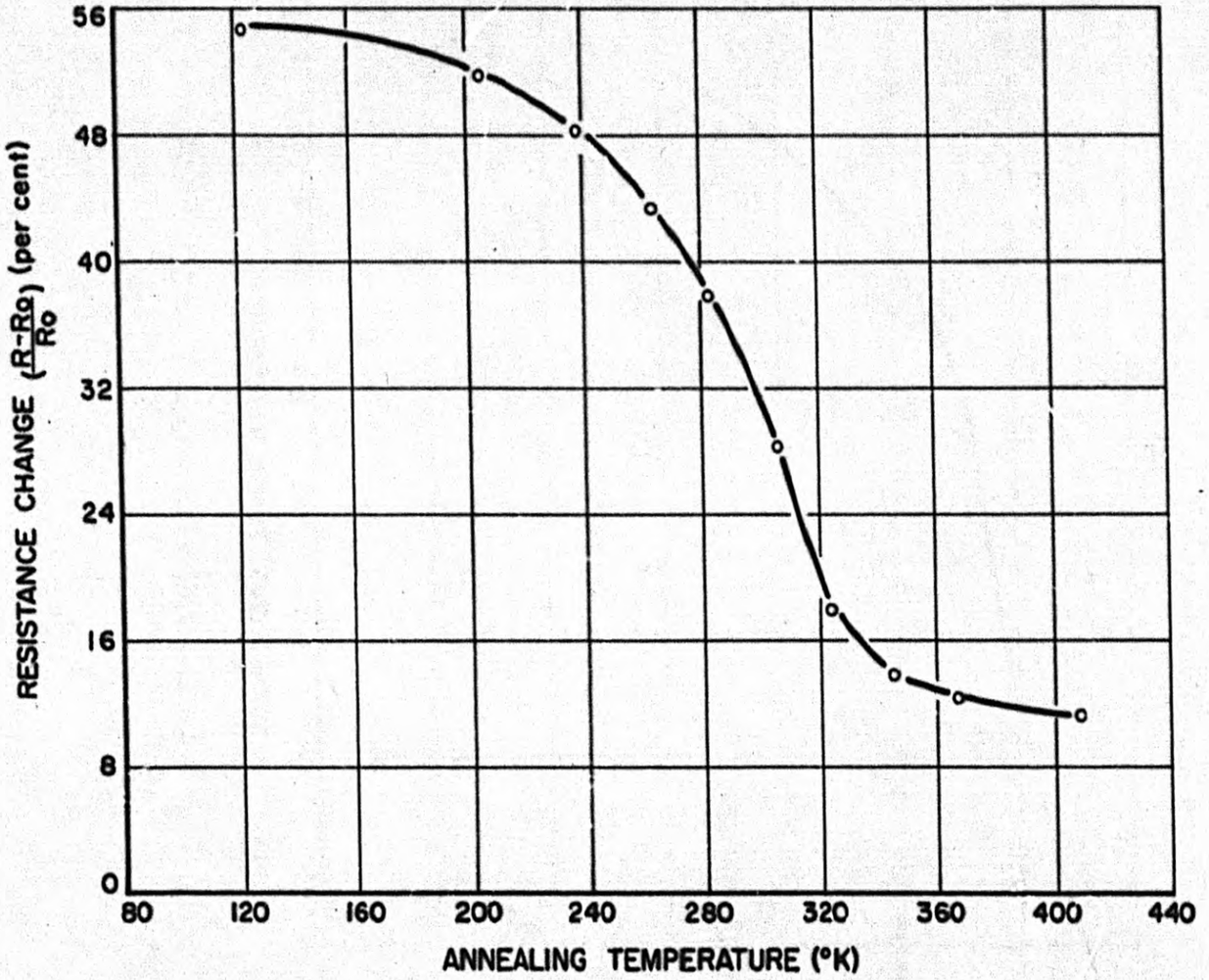

Fig. 15. Tempering Curve for Proton-Irradiated Thorium

D. Imperfections in Copper in Terms of Electrical Resistivity and Thermoelectric Power* - G. W. Rodeback

Certain types of imperfections in copper may be studied by including the Fermi energy dependence[16] of their electron scattering in the expressions for the electrical resistivity and the thermoelectric power. Measurements of electrical resistivity and thermoelectric power from 130° to 300° K have been made on various annealed states of cold-worked copper. Data were also taken from a sample bombarded at 150° K with 15 μamp-hr/cm^2 of 35 Mev alpha particles and subsequently annealed at room temperature. Two types of imperfections which contribute to the non-thermal scattering of conduction electrons are considered: fixed point scatterers whose scattering probability per unit time is assumed to have a one-half power dependence on Fermi energy, and boundary scatters whose scattering probability is assumed to be energy independent. If the imperfections due to cold work are assumed to be fixed point scatterers (perhaps vacancies) application of the free electron theory yields a Fermi energy constant over the ranges of annealing and temperatures of measurement. The same Fermi energy is approached above 200° K by the radiation-damaged copper if the imperfections are assumed to be boundary scatterers. This result is in agreement with the view that point scatterers (vacancies and interstitials) are annealed below room temperature.

E. Elastic Constants and Internal Friction - H. Dieckamp

More measurements have been made on cyclotron-irradiated 99.999 per cent pure copper wires and on wires given a slight amount of cold work.

Figure 16 shows the results of pulse annealing three of the cyclotron-irradiated samples. The temperature of irradiation was approximately -170° C and all subsequent storage and handling was done under liquid nitrogen. The measurements were made at liquid-nitrogen temperature by observing the free resonant frequency of a torsion pendulum whose period was about 1.2 seconds. The annealing time at each temperature was 15 minutes. These temperatures are correct to within 5° C and the precision of the frequency measurements is better than 0.05 per cent.

*Presented as an abstract to the American Physical Society for the Detroit-Ann Arbor Meeting.

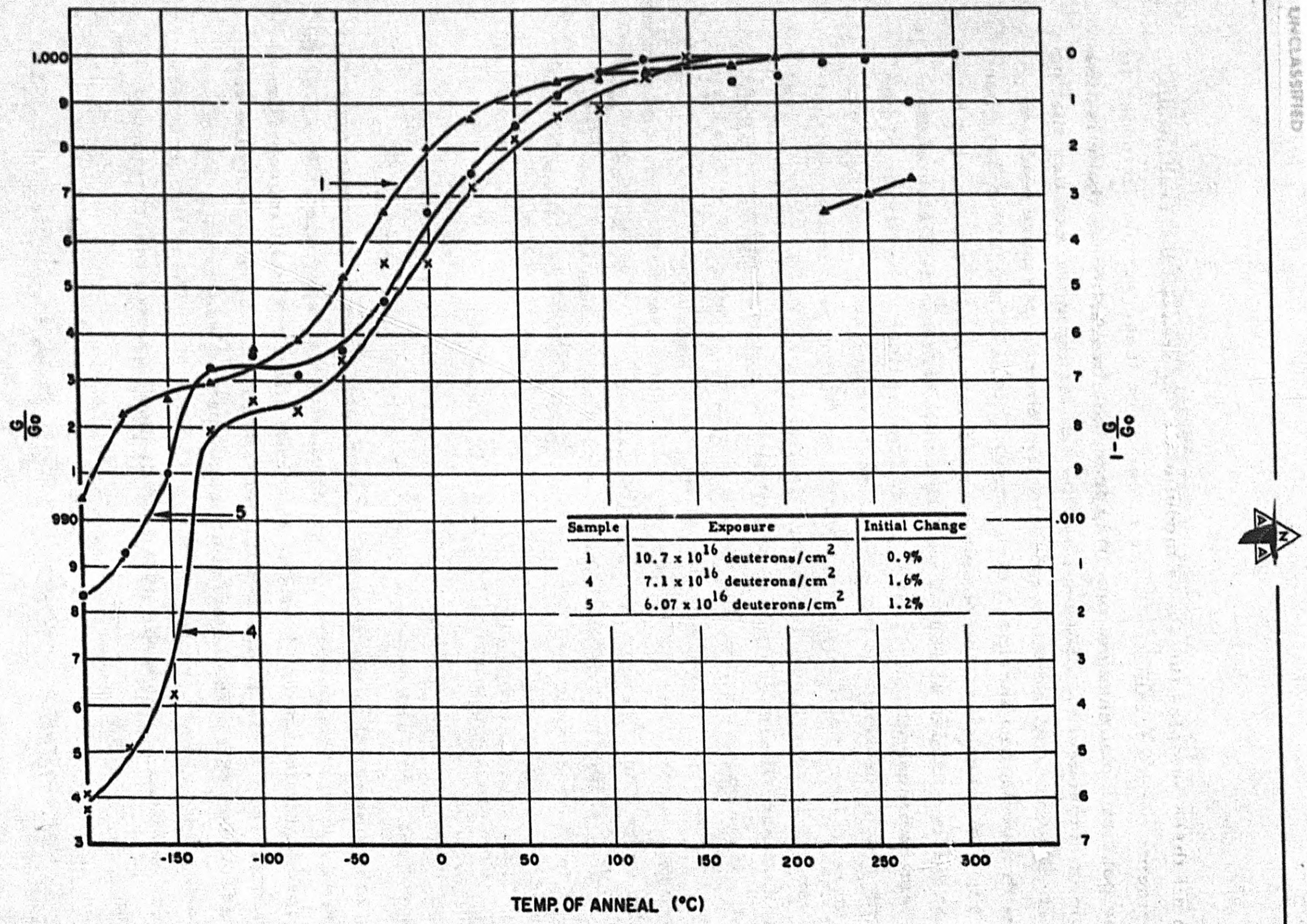

Fig. 16. Shear Modulus of Irradiated Copper

In all three samples the shear modulus was decreased by irradiation. Measurements before irradiation were not made on these samples in order to avoid the possibility of changes resulting from cold work. Since there is little indication of any annealing after heating to +150° C, the modulus after that point is taken as the undamaged value. Samples No. 5 and No. 4 show increasing change with increasing exposure, but Sample No. 1 does not follow this expected trend. Since this sample was in a higher intensity region of the beam it is suspected that the effective temperature of irradiation was sufficiently higher to account for the discrepancy.

Recent measurements on a sample given a very slight amount of cold work (surface shear strain of 0.8 per cent) showed that 50 per cent of the initial modulus decrease annealed at temperatures between +150° and +250° C. The absence of any significant or consistent annealing in this temperature range for the irradiated samples seems to substantiate the belief that the modulus decrease upon irradiation is not the result of cold work during handling.

Figure 17 shows the pulse annealing curves for one irradiated sample and two cold-worked samples. The data are plotted in a manner to emphasize the shape of the curves rather than the magnitude of the changes. The curves represent the percentage of the initial change remaining after each anneal as a function of the temperature of that anneal.

The model employed in attempting to explain the behavior of the shear modulus is one involving dislocations in conjunction with interstitials and vacancies. The dislocations seem to be necessary to account for the large changes resulting from cold work and for the rapid recovery at low temperature in both the cold-worked and the irradiated material. A mechanism involving the interaction of dislocations and point defects seems particularly appropriate since major portions of the modulus recovery takes place in those temperature ranges where one expects interstitials and vacancies to be mobile.

III. RADIATION DAMAGE IN INSULATORS

D. R. Westervelt and V. W. Martin

A. The Process: Colloid ⟶ F-Center

An estimate was made in the previous progress report[17] of the heat of

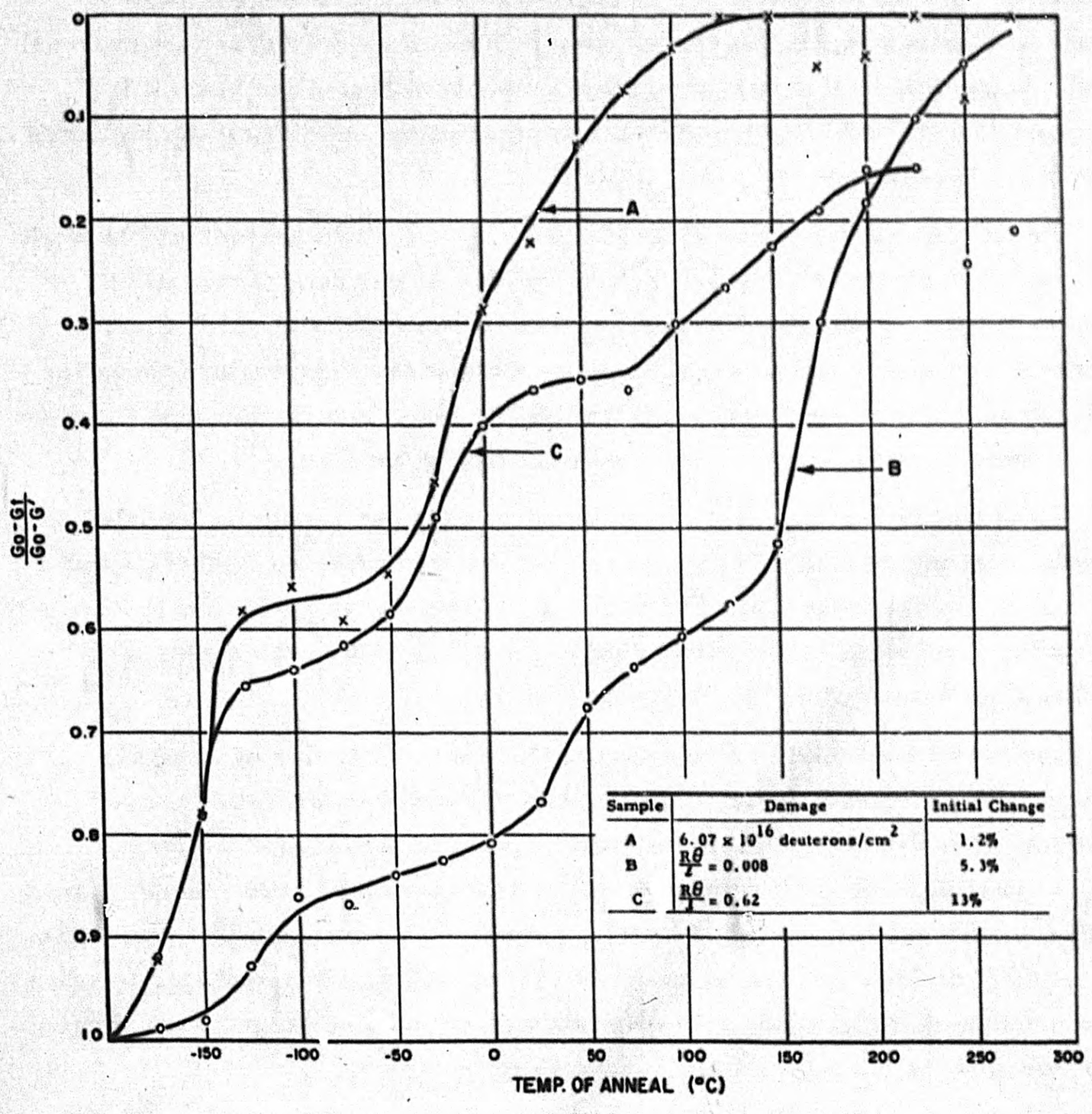

Fig. 17. Shear Modulus of Irradiated and Cold-Worked Copper (B)

reaction for the process in which a potassium atom is dissociated from a colloidal particle of potassium embedded in potassium chloride and added to the KCl lattice in the form of a K^+ ion and an F-center electron. A pair of vacancies is created simulatenously to maintain thermal equilibrium. It was assumed that the particle did not interact appreciably with the KCl lattice. The result obtained was 0.7 ev higher than an approximate empirical value, but the writer did not regard this difference as sufficient, in view of several uncertainties involved in the calculation, to serve as an argument against the theory that colloidal particles are partially responsible for the absorption spectra of suitably treated crystals.

This problem has been examined further in an effort to reduce the apparent disagreement betweem theory and experiment. In the course of this investigation several questions of fundamental importance have arisen, partially as a result of a recent paper[18] in the Russian literature concerning the mechanism of additive coloring.

A detailed analysis, therefore, has been completed of the reaction between colloidal alkali metal particles and excess alkali metal in the crystal in the form of F-centers. The analysis of this reaction required a slight revision of the Mott-Gurney derivation[19] of the ratio of F-centers to atom concentration in the vapor during additive coloring. It has been shown that ΔH, the heat of the colloid-F-center reaction observed by Scott and Smith,[20] is given by $Q + W_f$, where Q is the heat of vaporization of the alkali metal, and W_f is the work done in forming an F-center from the vapor.

The apparent disagreement between predicted and experimental values for ΔH has been shown to be largely eliminated if W_f is calculated from the most recent experimental data, namely, those of Scott and Smith, which lead to the value $W_f = -0.5$ ev. The value of W_f thus obtained has been compared with theory, and the discrepancy shown to be due most probably to inaccurate knowledge of $-\chi$, the electron affinity of KCl. It has been demonstrated that the new value of W_f leads to a qunatitatively correct prediction of the color-center concentration as a function of vapor pressure during the coloring process. A possible deviation of the coloring process from reversibility at high temperatures has been considered, and current experiments are designed to provide

the information required before the mechanism of coloring can be definitely established. It has been shown finally that colloidal particles of metal embedded in the KCl crystal most probably are in liquid form under a high hydrostatic pressure resulting from surface tension, their compression from this source being adequate to permit their formation in an unstrained KCl lattice. These conclusions will be discussed in detail in a forthcoming report.

B. Kinetics of the F-Center Coagulation Reaction

Probably the most important single question regarding the formation of colloidal particles during thermal annealing of crystals which contain F-centers is whether (a) the coagulation involves F-centers directly, or (b) there is a two-step process in which F-centers initially are destroyed (transformed into an intermediate center), and then a coagulation process occurs in which the centers resulting from the first process become aggregated into, presumably, colloidal metal. If the second mechanism prevails the process is similar to the situation which has been exploited successfully in the manufacture of photosensitive glass,[21] in which light is absorbed by activator ions. Thermal annealing destroys the activated centers with the formation of new centers, identified as an atomic dispersion of metal by their fluorescence. Continued annealing gives rise to colloidal aggregation and formation of a permanent visible photographic image. We believe that a similar process occurs in the alkali halides though they are presumably not activated by impurities.

Evidence that the thermal coagulation of F-centers is a two-step process has resulted from an analysis of the influence of light and temperature on the rate of transformation of F-centers to the R' and colloidal bands. The first process is greatly accelerated when the crystal is illuminated during annealing. In the dark this process occurs in KCl in a matter of minutes at 300° C, days at 150° C, and scarcely at all at 100° C. The thermal ionization energy for an F-center in KCl is about 2 ev. The rates observed in the dark, combined with this energy, lead to a provisional estimate of the frequency factor for thermal ionization of the F-center of the order of 10^{19} sec^{-1}, not unlike those derived for semiconductors by considering the density of available states. These results predict that at the higher temperatures employed by Scott[22] and his associates the destruction of F-centers during annealing should be completed almost instantaneously. Results obtained thus far confirm this expectation. Due to

the rapid transformations involved, it has been necessary to rebuild a furnace used in the spectrophotometer in order to obtain a shorter rise temperature. This work has been completed, and it now is possible to pulse to any temperature in the range from 25° to 300° C in less than 1 minute and to cool at a corresponding rate. The rate studies previously carried out with the old furnace are being repreated at present. An inspection of the data of Scott and co-workers suggests an activation energy of around 1.4 ev for the coagulation process, and a frequency factor closer to those normally observed in diffusion. We have concluded tentatively, then, that the R' band, which is transformed into the narrow colloidal band by further annealing (Fig. 18) comprises a significant early state in the thermal transformation of color centers.

It is significant that the peak of the R' band always lies at the same wave length, 735 mμ, while the colloidal-peak location depends on the annealing temperature and shifts to longer wave lengths as the temperature is raised. For a fixed F-center concentration we have found an approximately linear dependence of the colloidal peak wave length on annealing temperature from about 100° C to about 250° C, the shift toward longer wave lengths being about 60 mμ for this temperature interval. The rate of shift falls off rapidly at higher temperatures.

The Z-band (Fig. 19) in photochemically colored crystals evidently is identical to the R' band in additively colored crystals. We have previously attributed the Z-band to an intermediate center (zwischenzentren) rather than to colloidal particles, and this identification appears to gain support from the foregoing results. It may be wondered why a band corresponding to the R' rather than to the colloidal band is observed in the radiation-damaged crystals, even when they are annealed in the dark. One answer, and there may be more complicated ones, is that the crystals emit a considerable amount of blue-green light when heated so that it is in fact impossible to anneal them in the dark. In addition, the radiation damage is removed at a rate such that in the length of time necessary for aggregation into particles the damage is completely removed. Thus the "photographic image" in these crystals probably involves stable centers which are for smaller than the colloidal aggregates in photosensitive glass.

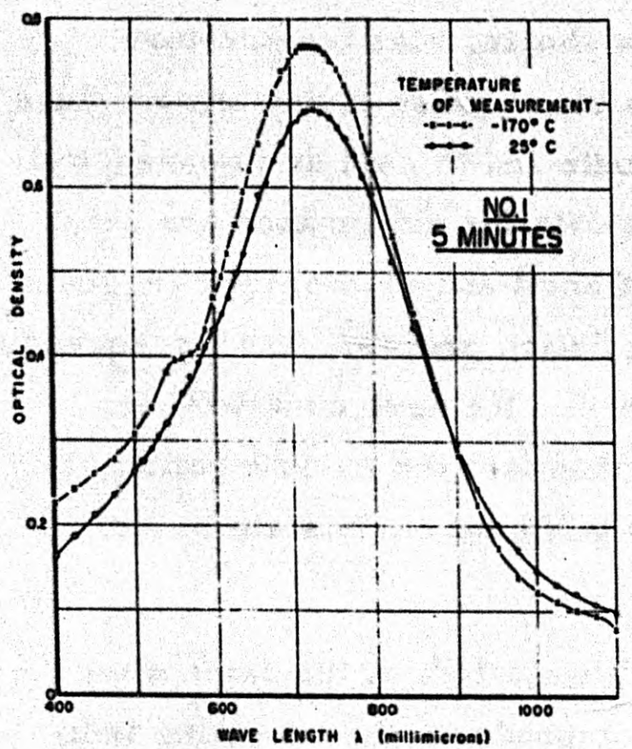

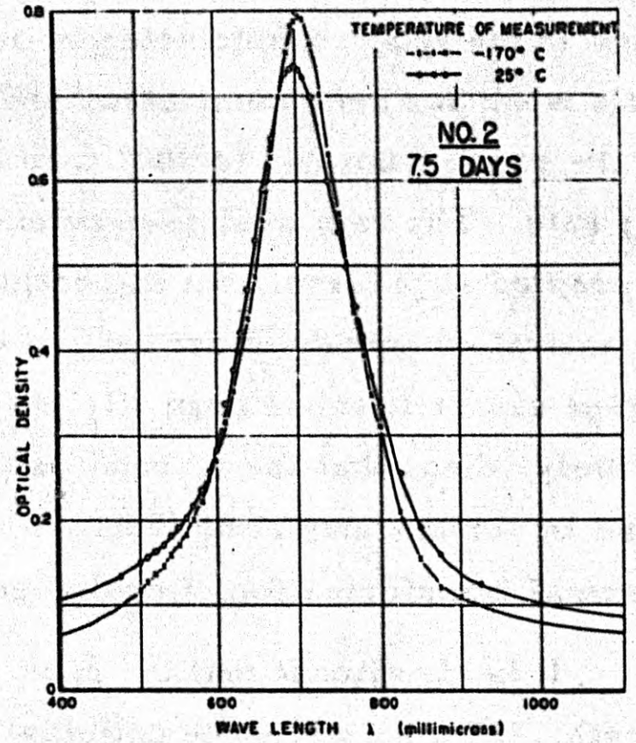

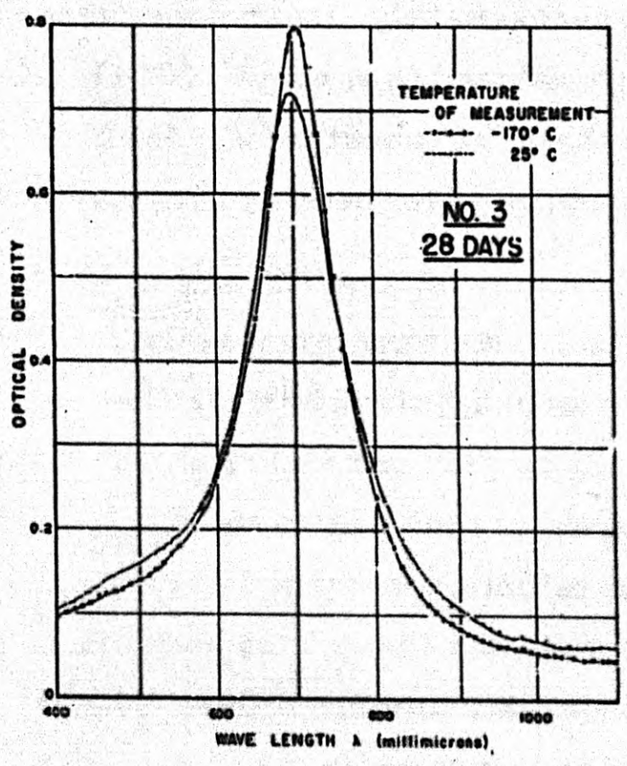

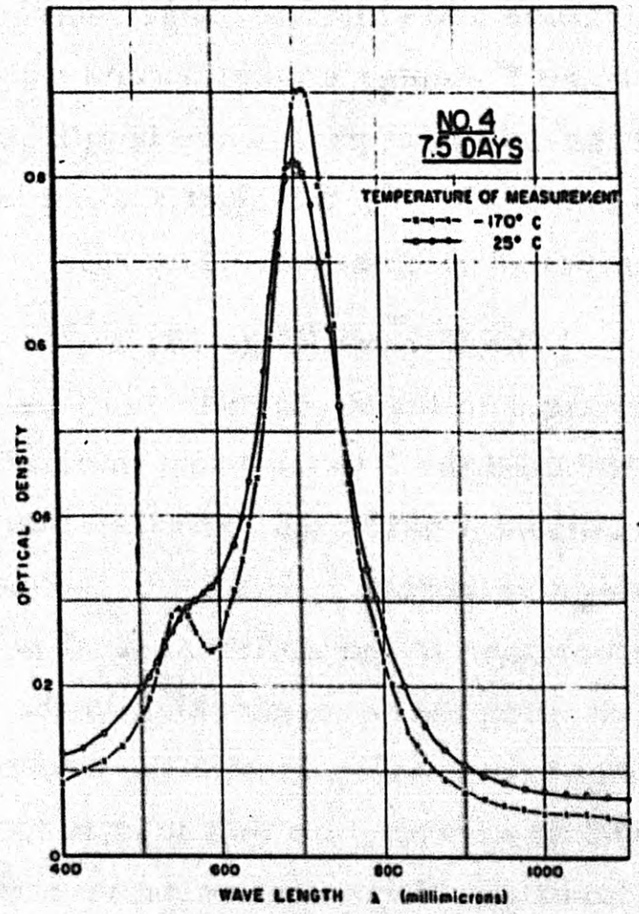

Fig. 18. Transformation of R' or Z-band (#1) to the Colloidal Band (#2, 3) by Prolonged Annealing. (#1, 2, 3 annealed in Light; #4 in Dark

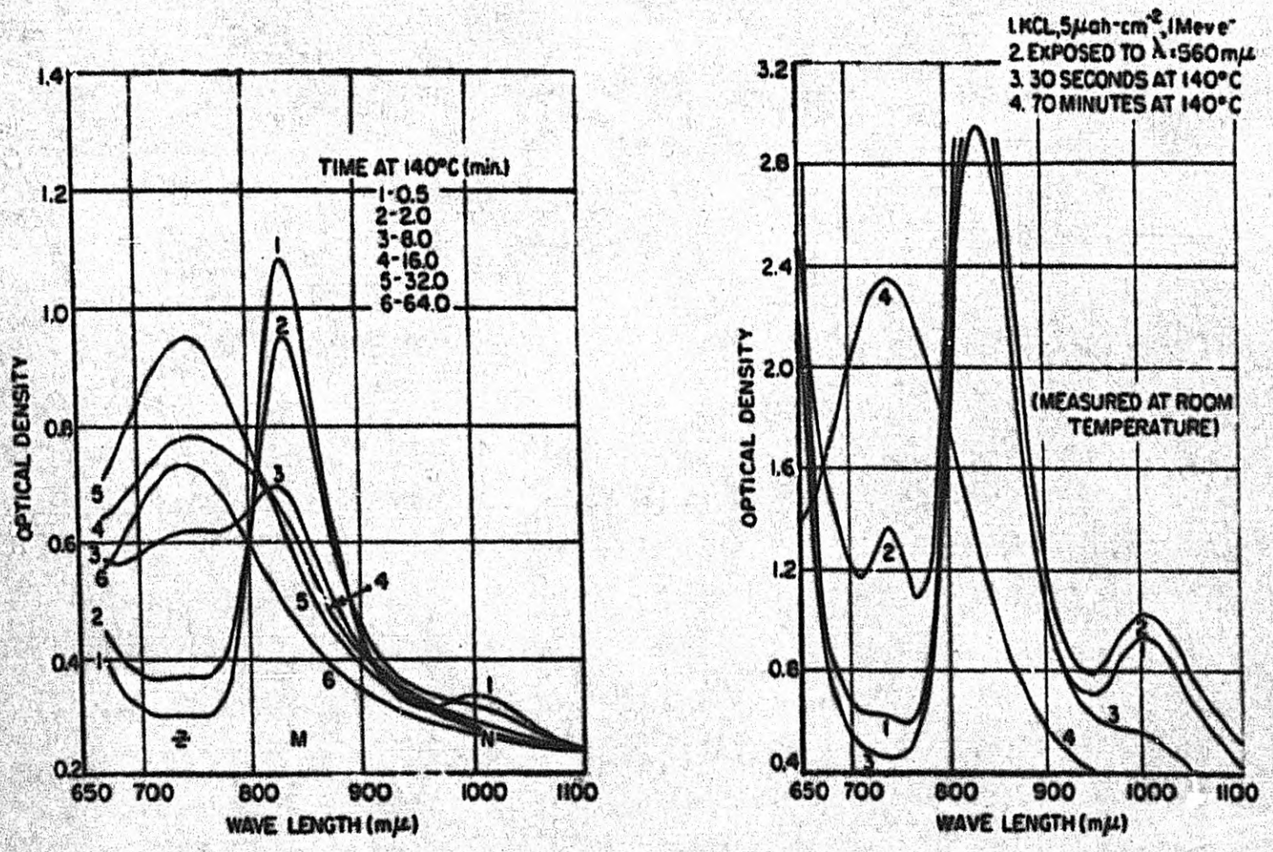

Fig. 19. Growth of the Z-band during Thermal Annealing of X-rayed and electron-bombarded KCl.

IV. IRRADIATIONS

A. Cyclotron Operation - A. Andrew

During this quarter, the 60-inch cyclotron at Crocker Laboratory was used a total of 166 hours for radiation damage studies. Irradiations were made in order to determine the effect of radiation on the following properties:

1. Thermoelectric power of graphite
2. Stored energy of graphite
3. Thermal conductivity of graphite
4. Disordering of Cu_3Au
5. Irradiation effects in thorium, uranium, and thorium-gold alloy
6. Displacement effects in impregnated graphite

B. Statitron Operation - H. Kenworthy

During the quarter ending March 31 the statitron was operated for a total of 585 hours. Of the total 425 hours were devoted to irradiations of chemical systems, primarily organic liquids, and 160 hours were devoted to irradiations of materials for solid-state studies.

REFERENCES

1. P. G. Klemens, Australian J. Phys. 6, 405 (1953).
2. A. W. Smith, Private Communication.
3. W. DeSorbo and W. W. Tyler, J. Chem. Phys. 21, 1660 (1953).
4. J. Krumhansl, J. Chem. Phys. 21, 1663 (1953).
5. N. S. Rasor and A. W. Smith, "Low Temperature Thermal and Electrical Conductivities of Normal and Neutron Irradiated Graphite," NAA-SR-862, June 1, 1954.
6. G. R. Hennig, J. Chem. Phys. 20, 1438 (1952).
7. G. R. Hennig and J. D. McClelland, "The Magnetic Susceptibility of Graphite Bromide," ANL-5064, June 8, 1953.
8. W. S. Gilbert, D. L. Clark and J. H. Pepper, "Thermoelectric Power of Graphite," pages 42 and 43 in "Radiation Effects Quarterly Progress Report, October-December, 1953," NAA-SR-909, May 15, 1954.
9. W. S. Gilbert and D. L. Clark, "In-PlaceMeasurements," page 17 in "Radiation Effects Quarterly Progress Report, July-September, 1953," NAA-SR-286, April 15, 1954.
10. R. L. Carter, "Asymptotic Aging Experiments," pages 26 through 32 in "Radiation Effects Quarterly Progress Report, July-September, 1953," NAA-SR-286, April 15, 1954.
11. R. L. Carter, "Measurement of Stored Energy During Quasi-Isothermal Annealing of Irradiated Graphite, I. Method and Preliminary Results," NAA-SR-288, April 15, 1954.
12. D. Hetrick and M. Mills, "Accidental Release of Stored Energy in a Hanford Reactor," NAA-SR-204, January 15, 1953.
13. J. A. Brinkman and W. S. Gilbert, "Annealing of Interstitial-Vacancy Pairs by Fission Fragments," pages 23 through 25 in "Solid State and Irradiation Physics Quarterly Progress Report, January-March, 1953," NAA-SR-251, October 8, 1953.
14. J. A. Brinkman and W. S. Gilbert, "Effects of Fission Fragments on Radiation-Damaged Metals," NAA-SR-262, November 15, 1953.
15. J. A. Brinkman, C. E. Dixon and C. J. Meechan, Acta Met. 2, 38 (1954).
16. G. W. Rodeback and W. P. Eatherly, Phys. Rev. 91, 237 (A) (1953).
17. D. R. Westervelt, "Radiation Damage in Insulators," pages 35 through 40 in "Radiation Effects Quarterly Progress Report, October-December, 1953," NAA-SR-909, May 15, 1954.
18. L. M. Shamousky, L. I. Rybakova and M. I. Gosteva, Doklady Academii Nauk USSR, 91, 67 (1953).
19. N. F. Mott and R. W. Gurney, Electronic Processes in Ionic Crystals, 2nd ed. (Clarendon Press, Oxford, 1948), p 144.

619-46

REFERENCES (Continued)

20. A. B. Scott and W. A. Smith, Phys. Rev. 83, 982 (1951).
21. S. D. Stookey, Ind. Eng. Chem., 41, 856 (1949).
22. A. B. Scott and W. A. Smith, loc. cit.

619-47